Response to the reviewers

Reviewer 1)

We thank reviewer 1 for their very insightful and constructive comments. We are certain that we substantially improved the quality of the paper thanks to this revision. We provide below a point-by-point response. The page and lines mentioned in the responses refer to the tracked-changes version of the revised manuscript.

Major comments

1- Comment #1 – page 2 lines 26-30: I would be a little more careful with your language here regarding the physical mechanisms underlying STT. I say this because purely quasi-isentropic mixing is only one mechanism whereby STT occurs. For example, cross isentropic mixing related to transverse circulations cannot be ignored even when you are talking about mixing events that begin as PV disturbances on isentropic surfaces (e.g., Langford JGR 1999). Another way to say this is that one needs to be cognizant of the fact that the actual exchange mechanism associated with wave breaking can take on a very different flavor depending on where you are on the globe. For example, quasi-isentropic mixing (at least in my mind), generally refers to the downgradient (scale-wise) mechanical mixing of filaments that occurs along isentropes. That is, there is not a whole lot of cross-isentropic mixing taking place (i.e., largely horizontal, but not so much in the vertical). This is typically the dominant mechanism in places like in the deep subtropics where STT is occurring on or near to the 350 K surface (e.g., Waugh and Polvani 2000 or Albers et al. 2016) or say in the interior of the stratosphere in the form of the south-north "eddy mixing" portions of the BDC.
In the extratropics on the other hand, and in particular in association with the polar front, wave breaking begins with three dimensional folding/corkscrewing of the tropopause along isentropes, but in this case, a great deal of the mass exchange is associated with vertical turbulent mixing/erosion and diabatically induced cross-isentropic mixing of the fold itself. These are the ideas discussed in Shapiro (1980), Langford and Reid (1998), Wernli and Sprenger (2007), and Sprenger et al. (2003) (as well as the Stohl STACCATO paper you reference). Now, I'm not suggesting that you go into as much detail as the Wernli/Sprenger papers, i.e., it's probably not relevant for your paper to spend time discussing the intricacies of how wave breaking STT is manifest as folds vs. streamers vs. cutoff lows; however, I do think that you should be a little more precise with your discussion of the physical mechanisms responsible for mass exchange and the fact that in different regions of the globe, there are different processes at play.

Thank you for this nice overview summary of STT processes. We rewrote this Introduction paragraph, clarifying the different processes that take place in subtropics and extratropics (P2 L26-34).

2- Comment #2 – page 7 lines 15-25: I must be missing something here, because when I look at Figure 5, I do not see common behavior across all models, rather EMAC and GEOS have one behavior in the NH UTLS (positive trends), while all the other models (WACCM, CMAM, etc.) have a negative trend. This seems like a pretty notable difference that needs to be addressed.

This is true, this difference should be highlighted. We included this (P7L29-31), and we also mentioned that this is probably due to a larger contribution from ozone recovery (ODS) that cancels

the negative trends expected from tropopause rise (GHG) in these two models, as can be concluded from Fig. 11, even though the output for these two models in particular is not available.

Comment #3 – page 7 lines 15-25: This question is related to my comment #2 immediately above. In Fig. 5, the negative trends in the tropical stratosphere are easily explained via the enhancement of the BDC, so that portion of your physical explanation seems fine. However, when you state that "...as stated above, these trends around the extratropical tropopause....", it is unclear which explanation above you are referring to because it would seem that the rise in the tropopause (which is not particularly large) cannot alone explain the bulk of the negative trends in O3S that extend all the way down to 500 hPa in the extratropics. This would leave isentropic mixing and the residual circulation to explain the trends. I can think of a couple options here, but some of them don't seem to be consistent with your streamfunction plots in Figs. 7 and 10.

For example, your streamfunction plots show that the residual circulation accelerates coming up and out of the tropics (as expected if the deep branch of the BDC accelerates), but then there is a notable region of deceleration between 30o-80o N between 10-15 km (depending on the model). Now, I'm not sure how to label this region of negative streamfunction trend though it would seem that it could qualify as being part shallow branch and part of the lowermost portion of extratropical deep branch (perhaps this distinction is a bit ill-posed), but regardless of the what aspect of the BDC it is, the fact that it weakens could plausibly mean that less ozone is being transported downwards into the UTLS, hence helping to explain the decreasing ozone trend right at or above the tropopause. And if there is less ozone around the tropopause, then there is less ozone to be mixed via tropopause folds etc into the extratropical mid-to-upper troposphere, which would in total help explain the overall negative extratropical UTLS trend. However, all of the models have the same qualitative streamfunction trend, yet as I stated above, EMAC and GEOS do NOT show the negative O3S trend. Thus, it would seem difficult to explain the extratropical UTLS trend via the residual circulation (your Fig. 8 seems to confirm this conclusion because again, all of the models have the same qualitative advective changes, yet not all models get the same extra. UTLS O3S trend).

That leaves mixing to explain the trends. However again, the eddy transports don't (at least to my eye) seem to help explain why there is a negative trend in some models but a positive trend in others.

Please help me and other readers to understand what is physically going on here.

Our argument is that changes in tropopause height, small as they are on average, lead to substantial changes in the tracer concentrations. In Abalos et al. 2017 JAS we showed this to be the case for the tropospheric tracer e90, and here we present the same argument for the stratospheric tracers o3S and st80. To highlight this point, we now mention that the band of negative trends in the extratropical UTLS disappears when tropopause-relative altitude coordinate is used. This strong influence of tropopause rise can be explained in two ways (i.e., through two mechanisms which we think are acting together). First, concomitant with the tropopause rise there is an (upward) expansion of the troposphere, which implies that the air around the tropopause becomes more tropospheric-like, and consistently the concentrations of stratospheric tracer decrease. In addition, we argue, following Abalos et al. 2017 JAS, that the upward shift of the tropopause is linked to changes in static stability which in turn modify the wave propagation and dissipation conditions, resulting in modified mixing strength. We do observe some signal of this enhanced mixing in the TEM eddy transport term, but the lack of consistency among models, and the fact that negative trends extend to lower levels than the mixing trends, prevents us to be conclusive about this last mechanism. Thus, we have lowered

the tone attributing these trends to changes in mixing and mentioned the first mechanism, also following suggestions of the other reviewer. These changes can be found in several places in the paper: P7L14-21, P10L34-35, P15L1-9. Regarding the difference between models, it is likely due to different degrees of cancellation between the opposite effects of ODS and GHG in different models, as mentioned in the response to your comment #2.

Comment #4 – page 9 line 11: I'm not sure I agree with your statement that Fig. 9 shows that ADV is the same in all models. I would agree that it is qualitatively the same in the UTLS between -30o-30o in all models. However, the extratropical UTLS shows two different behaviors (CMAM and EMAC vs. GEOS and WACCM). And again, this seems to point to the fact that you cannot explain the different O3S trends in the extratropical UTLS shown in Fig. 5 via advection, because while in Fig. 5 EMAC and GEOS showsimilar behavior (positive trend), WACCM and CMAM show a negative trend, yet in Fig. 9, WACCM and GEOS have similar extratropical patterns (somewhat complicated, but consistent), while CMAM and EMAC show similar behavior (essentially no trend in the extratropics). Now I realize that s80 and O3S are different tracers, but given that they are both being advected via the same dynamics, it would seem that there should be some underlying commonality that can help rectify the different extratropical UTLS O3S patterns between the different models. Thus, it would help if the differences were at a minimum mentioned and hopefully the implications of these differences explained.

We agree with the reviewer that this should be explained. The issue here is that the st80 climatology in the lower stratosphere in CMAM and EMAC is different from the other of the models, as can be seen in Orbe et al. 2018 ACP, supplementary material Figure S2. More specifically, while GEOSCCM and WACCM present positive st80 trends in the extratropical lower stratosphere (as expected from accelerated BDC downwelling), CMAM and EMAC present negative trends in this region. The enhanced downward advective transport of st80 into the polar troposphere found in GEOSCCM and WACCM is due to the increasing tracer concentrations in the lowermost stratosphere (i.e., a larger reservoir of st80 to be transported downward). The same mechanism applies to O3S: the accumulation of O3S in the lower stratosphere leads to enhanced downward advective transport into the troposphere. All the models show this consistent behavior for O3S (Fig. 7). We have explained this issue in more detail on P10 L8-15.

Minor comments

Comment #1 – page 7 line 17: Where you state "...are attributed to changes...", instead of 'changes' can you be more precise and state what the change is? A 'decrease'?

Consistent with our response to comment #3, we have lowered the tone on the attribution to mixing and now we changed the sentence to: "As stated above, the negative trends in the extratropical UTLS are a fingerprint of the rise of the tropopause."

Comment #2 – Figures: A bunch of your figures are missing pressure labels on their axis. Some figures have the labels, while other don't. Personally I find the pressure labels helpful, so perhaps you can add them for all figures?

We added pressure levels on all panels of Figs. 7, 8, 9, 10.

References:

Langford, A. (1999). Stratosphere-troposphere exchange at the subtropical jet: Contribution to the tropospheric ozone budget at midlatitudes. Geophysical Research Letters, 26(16), 2449–2452.

Shapiro, M. (1980). Turbulent mixing within tropopause folds as a mechanism for the exchange of chemical constituents between the stratosphere and troposphere. Journal of the Atmospheric Sciences, 37(5), 994–1004.
Langford, A., & Reid, S. (1998). Dissipation and mixing of a small-scale stratospheric intrusion in the upper troposphere. Journal of Geophysical Research, 103(D23), 31,265–31,276
Waugh, D. W., & Polvani, L. M. (2000). Climatology of intrusions into the tropical upper troposphere. Geophysical Research Letters, 27(23), 3857 – 3860.
Albers, J. R., Kiladis, G. N., Birner, T., & Dias, J. (2016). Tropical upper-tropospheric potential vorticity intrusions during sudden stratospheric warmings. Journal of the Atmospheric Sciences, 73(6), 2361–2384.
Wernli, H. and M. Sprenger (2007): Identification and ERA-15 Climatology of Potential Vorticity Streamers and Cutoffs near the Extratropical Tropopause, Journal of the Atmospheric Sciences.
Sprenger et al. (2003): Tropopause folds and cross-tropopause exchange: A global investigation based upon ECMWF analyses for the time period March 2000 to February 2001. J. Geophys. Res.

Reviewer 2)

We acknowledge the careful and constructive review which has contributed to notably improve the paper. We provide a point-by-point response below.

Major comments:

(a) The use of TEM budget analysis.
Besides that the advective transport shows significant contribution to the subtropical tongue of st80, I feel like the TEM budget analysis does not help that much on interpreting the spatial distribution of STT trend inferred by two stratospheric tracers (O3S and st80). Firstly, I am wondering how consistent, in terms of the spatial distribution, between the trend of tracers (unit: ppbv/decade) and the combined tracer tendency from advective-diffusive processes estimated in the TEM framework (unit: ppbv/day)? My first impression is not so much. For example, none of the advective transport or eddy mixing or combined can explain the negative trend of O3S in the NH extratropics especially the part below the tropopause. Moreover, the prominent positive trend of O3S in the SH extratropics in contrasting to the negative trend in the NH extratropics is suggested by neither advective transport nor eddy mixing of O3S. Therefore, multiple things need to be checked, which include (i) how much the trend is captured by tracer concentration differences between the present and the future, (ii) how much the difference is captured by the resolved transport approximated by the TEM framework. These checks have mostly been done in Abalos et al. (2017) so should not be problems to additionally apply to the stratospheric tracers. Also, Abalos et al. (2017) used tracer concentration difference (see their equation 2) to interpret the future trend of e90, but I am not so sure how valid it is for O3S if there is also a change in O3S lifetime τ (lifetime is fixed for e90 and st80). In sum, I think interpretation of TEM budget analysis should use more cautions if the leading spatial features of tracer trend (especially those near the tropopause) cannot be captured by this framework.

Thank you for this comment. Regarding (i): we have checked that the trends and the future minus past difference in the tracer concentrations are highly consistent (not shown). Regarding (ii): we do not attempt here to provide a quantitative estimate of the contribution from each term to the net tracer trends. In order to do this, we should include all the other terms in the balance in addition to the resolved transport terms (advection and eddy transport): non-resolved transport terms (convection, diffusion, transport by subgrid-scale waves) and the chemical tendency term (likely important for O3S). Still, there would be a residual that prevents closing the budget, due to the numerical issues such as those listed in Abalos et al 2017 JAS, and their equivalent for other models. Nevertheless, the two resolved transport terms give valuable information on the effects of these two types of transport mechanisms on the tracer trends. In particular, the advective transport term helps illustrate the effects of the residual circulation trends on the tracers STT, which we consider a key point of this paper. These effects would be hard to mentally picture from the trends in the circulation alone (Fig. 7). In addition to the subtropical tongues mentioned by the reviewer, the NH polar downwelling trends are evidenced, which we have now emphasized in the revised version of the paper.

Finally, as the reviewer correctly states, we cannot apply Eq. (2) from Abalos et al. 2017 to O3S, given that it has time-varying chemical tendencies. This is why we have expressed the TEM trends in ppbv/day (difference between transport terms in the future minus past), instead of converting them to ppbv, as was done in the 2017 paper for e90.

We are confident that the explanations included in the revised manuscript ensure that the results regarding the TEM terms are interpreted correctly, accounting for their limitations. See P11 L5-10.

(b) Interpretation of stratospheric tracer trends at the extratropical tropopause.
The paper has shown positive trend of e90 and negative trends of stratospheric tracers over the extratropical tropopause region, except the O3S in the SH extratropics where the authors argued recovery of ozone hole matters. I highly agree with the authors this feature is associated with the upward shift of tropopause. However, I am not so sure for their additional claim on enhanced isentropic mixing on the tropopause. In my opinion, without any change in the strength of mixing at the tropopause, an upward shift of tropopause alone can already cause the increase (decrease) of tropospheric (stratospheric)tracers in the tropopause region. Specifically, as the tropopause shifting upward, tropospheric tracers (e.g., e90) can move further upward before encountering the transport barrier by tropopause and thus more tropospheric tracers near the tropopause region which the positive trend tends to maximize in between the old and new tropopauses (see Fig. 4). By contrast, as the tropopause shifting upward, downward transport of stratospheric tracers encounters earlier with the tropopause barrier, and thus less stratospheric tracers near the tropopause region with the negative trend also maximizing in between the old and new tropopauses, as shown in Figs. 5 and 6. The enhancement of isentropic mixing on the tropopause could indeed amplify this effect, but given the fact that models are not showing consistent results about the eddy mixing component (briefly noted in the manuscript) plus the results of eddy mixing component are much more noisy, I don't think a strong conclusion on enhanced isentropic mixing on the tropopause can be made. Finally, as noted earlier in (a), neither advective transport nor eddy mixing seem to reflect the prominent negative trend of stratospheric tracers in the NH extratropics, particularly the part below the tropopause. Therefore, I suspect that the TEM budget analysis may not show up the effect of tropopause rise on extratratropic tracer transport.

We agree with the reviewer that we have probably overstated the role of changes in mixing on the extratropical UTLS trends, given the uncertainty in this term. We understand that there is likely a contribution directly from the fact that the troposphere expands. To address this comment, we have restated the interpretations in the paper on the extratropical UTLS trends, stressing the uncertainties in the mixing term and including this second mechanism. Moreover, we have emphasized the tropopause rise as a key factor for the extratropical UTLS trends, since this feature is the driver behind both mechanisms. These changes are found in several parts of the manuscript (P7L14-21, P10L34-35, P15L1-9).

(c) Lack of mechanism interpretation on inter-model differences of STT.
The authors give some good examples of comparing trends of tropospheric-column averaged tracer concentration for O3S and st80 in Section 3.1 and 5 to highlight the inter-model differences, which is "one great merit" of looking at inter-model comparison project. However, when coming across the discussion of mechanism in Section 4, none of these inter-model differences are noted again, so is the spatial distribution in Section 3.2. It is good to focus on common features that are supported by most of models, but the inter-model differences could also bring some interesting insights. For example, models like CMAM show larger tropospheric appearance of st80 than models like WACCM and GEOSCCM, which are likely due to stronger subtropical tongue in CMAM than those in WACCM/GEOSCCM and therefore link to stronger lower BDC and upper HC overturning in CMAM than those in WACCM/GEOSCCM (see Fig. 7). This again highlights the importance of advective transport for STT of st80. The inter-model differences in O3S are more complicated but a brief discussion may be helpful.

We agree with the reviewer that the inter-model spread can be used to extract information on the mechanisms, and this is one merit of multi-model studies. Accordingly, we decided to remove the scatter plots against tropopause altitude because they were not providing any information on the processes (see response to next comment). In their place, we show now plots of STT against tropical upwelling trends. In this way, we use the inter-model spread to illustrate the influence of the BDC on STT, stressing this key point of the paper. Note that we also merged the figure for the stratospheric tracers with that for e90 (old Figs. 2 and 3) and included them in the new Fig. 2, in order to reduce the number of figures from 13 to 12. See related discussion on P6 L18-36.

Minor (and technic) comments:

P1: Institutions 4 and 5 should switch place.

Done, thank you for noticing the error.

P6L15-P6L19: From later results, it seems that the tropopause rise is more related to variations in STT over the extratropics instead of the global STT shown by tropospheric burden of these stratospheric tracers. The global STT is likely controlled by other processes (e.g., subtropical tongue due to overturning circulation in the UTLS for st80). In short, I am not surprised that the correlation is weaker for tropopause rise than climate response and I doubt how confident the authors can argue tropopause rise act as an important mediator for the global budget.

We agree with the reviewer on this point. This comment, together with Major comment (c), led us to rethink the figures of the paper as described in the response to comment (c). Indeed, the old Fig. 2 showed the negative result that tropopause altitude trends are not correlated with global STT trends. The changes introduced in Fig. 2 allow to highlight two important results of the paper: 1) models with larger climate sensitivity present larger STT trends, and 2) STT trends are connected to BDC trends.

P7L34-P8L1: The authors noted some differences about spatial distribution between O3S and st80. I think this should be highlighted more often in the manuscript to warn readers that interpretation of O3S should use more cautions as both variations in stratospheric chemistry andsource distributions could yield different behaviors from st80. Also, I suggest the authors to insert cross-section maps for climatological O3S and st80 distribution (either a new figure or superimposed in existing figures as contours) so that readers can have a better idea on how the future changes in tracers compare to the climatological distribution.

Thank you for the suggestion. We have highlighted these differences more often in the manuscript and we added climatology contours in Figs. 3, 4 and 5.

P8L2-P8L5: I think st80 in upper-troposphere deep tropics can also be interpreted by later results of advective transport and eddy mixing. From Figs. 9 and 10, the advective transport of st80 in deep tropics generally shows negative trend while the eddy mixing shows positive trend. The eddy mixing component seems to have a larger trend than the advective transport so that the net compensation outcome shows the positive trend. For CMAM model in which the negative trend by advective transport is so strong in deep tropics that cannot be fully compensated by eddy mixing shows a net outcome of local negative trend. In sum, I agree with the authors that variations of st80 in deep tropics are related to enhanced diffusion on the tropopause but not quite sure whether the tropopause altitude playing a role here. As mentioned in the major comments, in my opinion, tropopause rise works better for extratropical STT variations which its influence seems not to be captured by the TEM diagnostics.

We agree with the reviewer that it is not clear that tropopause altitude is the only factor leading to differences in deep tropics st80 trends among models. However, we are not confident that the TEM analyses help us understand the model spread. In fact, as mentioned in the response to your comment #1, we prefer not making claims on relative roles of the two transport terms on the tracer trends, since we do not close the budget. On the other hand, looking at the climatological concentrations of st80 now plotted in Fig. 5, it becomes evident that the two models with stronger trends in the deep tropics (CMAM and EMAC) are also those that also have larger climatological concentrations in this region. This suggests that in these models there is more cross-tropopause diffusion of the tracer into the troposphere. The reason for this could be the different transport/diffusion properties of the models, though a higher tropical tropopause, closer to the 80 hPa source of the tracer, likely contributes to magnify this effect. We have clarified this in the manuscript (P8 L20-25).

P8L14: las -> last

Changed.

P8L15: Polvani et al. 2019 -> Polvani et al. (2019)

Changed.

P9L2-P9L3: This part reads so similar to earlier part of ozone recovery-related variations in residual circulation, so it confuses initially. I suggest to diffrentiate at the beginning about the double effects of ozone recovery on STT of O3S: (i) weaken the downwelling of residual circulation leading to less polar O3S accumulation by transport, and (ii) increase polar ozone concentrations. Effects of (i) dominates above 20 km so O3S shows negative trend while effects of (ii) surpass below 20 km so that O3S shows positive trend suggesting stronger STT of O3S at polar regions.

Changed, thank you.

P9L12-P9L13: Although both O3S and st80 highlighting the subtropical tongue for transport in the UTLS region, there are some differences about their advective transport: (i) transport in the deep tropics which is likely due to differences in source, and (ii) subtropical tongue seems to intrude more vertically as for st80 than O3S. Do you have an idea on why is so?

Regarding (i), we think it is likely due to differences in source regions, see response to your previous comment about P8L2-P8L5. Regarding (ii), considering that the advective term is -v* dX/dy – w*dX/dz, this difference has to be due to the different vertical/meridional gradients in the two tracers, since the residual circulation is the same. Specifically, for st80 the vertical term dominates over the meridional more than for O3S. However, we agree that this is not obvious from simply looking at the climatological contours in Figs. 4 and 5.

P9L32-P10L1: As noted in the major comments, I suspect how strong this conclusion can be given that the TEM diagnostics seems to fail to capture the effects of tropopause rise on STT.

We have included the direct effect of the tropospheric expansion argued by the referee as an additional driver of the extratropical UTLS trends.

P10L26-P10L29: Would this be clearer if additional lines for the corresponding RCP6.0 cases

are added in Fig.11(a-d)?

Yes, definitely, thank you for the suggestion. As we added them, we realizedthat, in order to compare runs of the same model it is best to compare the st80 without standardizing, to avoid losing information. So we changed this, and now all the models show a stronger STT trends for the more extreme scenario for both tracers, as expected. By having both curves in the same plot, we also realized that the change in stratospheric-to-total ozone ratio is not significant, and we mentioned this in the manuscript. Overall the interpretation of this figure is much clearer now.

fGHG vs fODS: I am interested in seeing how much the addition of fGHG+fODS can explain the full trend seen in Figs. 5 and 6. Also, I think for both O3S and st80, the fODS explains more on the full trend response of STT than fGHG, which could be pointed out at the beginning of P11L14.

We would like to clarify that these runs are not exactly additive, because they are not single forcing runs, but all forcing-minus-one runs. Adding them would imply adding twice some effects (such as aerosol, for instance). Nevertheless, it is insightful to examine the relative contribution of each single forcing (GHG and ODS) to the total trends, which can be done by comparing the timeseries, as shown in Fig. R1. From this figure it is clear that, in the case of st80, climate change is responsible for the trend in STT, and ODS do not play any significant role. In the case of O3S, the opposite is true for ACCESS and NIWA, i.e., ozone recovery completely dominates over the effect of GHG. In CMAM however, both effects have similar magnitude. These are indeed interesting results and we have included them in the paper thanks to the referee's suggestion. P13 L9-12.

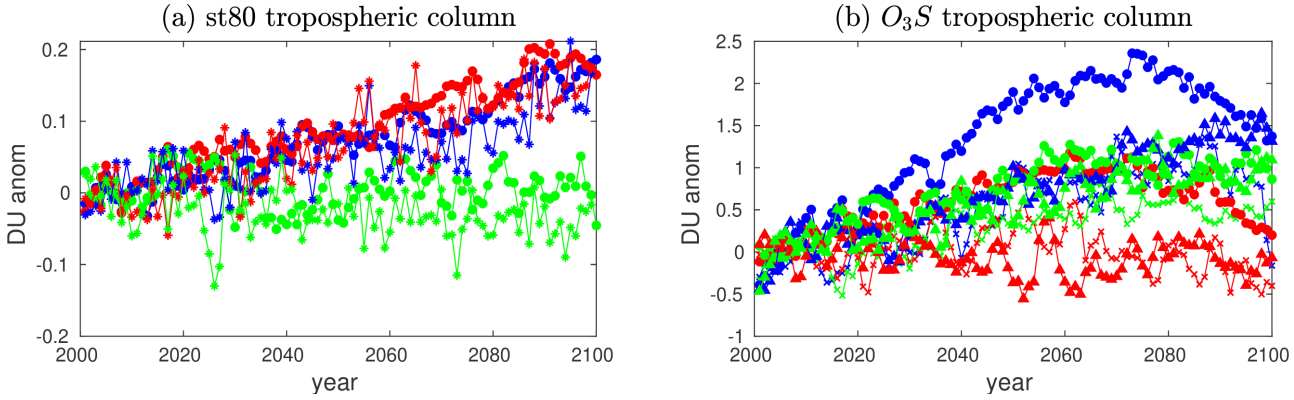

Figure R1. Timeseries of st80 (a) and o3s (b) tropospheric columns for the REF-C2 runs (blue) compared to tehe SEN-C2-fODS (red) and SEN-C2-fGHG (green). The different symbols represent different models: CMAM (circles), WACCM (stars), ACCESS (crosses), NIWA (triangles). In both panels are represented anomalies with respect to the average of the first ten years.

P11L23: is "the" strongest

Changed.

P11L24-P11L25: Should these cross-references be Fig. 12?

Yes, thank you. Changed.

P12L5: Polvani et al. 2019 -> Polvani et al. (2019)

Changed.

P13L10: this region -> the extratropical lower stratosphere

This sentence is changed in the new version.

Future trends in stratosphere-to-troposphere transport in CCMI models

Marta Abalos[1], Clara Orbe[2], Douglas E. Kinnison[3], David Plummer[4], Luke D. Oman[5], Patrick Jöckel[6], Olaf Morgenstern[7], Rolando R. Garcia[3], Guang Zeng[7], Kane A. Stone[8, 9, *], and Martin Dameris[6]

[1]Department of Earth Physics and Astrophysics, Universidad Complutense de Madrid, Madrid, Spain
[2]NASA Goddard Institute for Space Studies, New York, NY, USA
[3]National Center for Atmospheric Research, Boulder, CO, USA
[4]Climate Research Branch, Environment and Climate Change Canada, Montreal, Canada
[5]NASA Goddard Space Flight Center, Greenbelt, MD, USA
[6]Deutsches Zentrum für Luft- und Raumfahrt (DLR), Institut für Physik der Atmosphäre, Oberpfaffenhofen, Germany
[7]National Institute of Water and Atmospheric Research (NIWA), Wellington, New Zealand
[8]School of Earth Sciences, University of Melbourne, Melbourne, Victoria 3010, Australia
[9]ARC Centre of Excellence for Climate System Science, University of New South Wales, Sydney, New South Wales 2052, Australia
[*]Now at: Department of Earth, Atmospheric and Planetary Sciences, Massachusetts Institute of Technology, Cambridge, MA, USA

Correspondence: Marta Abalos (mabalosa@ucm.es)

Abstract. One of the key questions in the air quality and climate sciences is how will tropospheric ozone concentrations change in the future. This will depend on two factors: changes in stratosphere-to-troposphere transport (STT) and changes in tropospheric chemistry. Here we aim to identify robust changes in STT using simulations from the Chemistry Climate Model Initiative (CCMI) under a common climate change scenario (RCP6.0). We use two idealized stratospheric tracers to isolate changes in transport: stratospheric ozone (O_3S), which is exactly like ozone but has no chemical sources in the troposphere, and st80, a passive tracer with fixed volume mixing ratio in the stratosphere. We find a robust increase in the tropospheric columns of these two tracers across the models. In particular, stratospheric ozone in the troposphere is projected to increase 10-16% by the end of the 21st century in the RCP6.0 scenario. Future STT is enhanced in the subtropics due to the strengthening of the shallow branch of the Brewer-Dobson circulation (BDC) in the lower stratosphere and of the upper part of the Hadley cell in the upper troposphere. The acceleration of the deep branch of the BDC in the NH, and changes in eddy transport contribute to ~~increase~~ increased STT at high latitudes. ~~The idealized tracer st80 shows that these STT changes are dominated~~ These STT trends are caused by greenhouse gas (GHG) increases, while phasing out of ozone depleting substances (ODS) does not lead to robust ~~STT~~ transport changes. Nevertheless, the ~~increase of~~ decline of ODS increases the reservoir of ozone in the lower stratosphere, which results in enhanced STT of O_3S ~~concentrations in the troposphere is attributed to GHG only in the subtropics. At~~ at middle and high latitudes~~it is due to stratospheric ozone recovery linked to ODS decline~~. A higher emission scenario (RCP8.5) produces ~~qualitatively similar but~~ stronger STT trends, with ~~changes~~ increases in tropospheric column O_3S more than three times larger than those in the RCP6.0 scenario by the end of the 21st century.

1 Introduction

Ozone is most abundant in the stratosphere, and its presence is crucial for protecting life on Earth from ~~the~~ harmful solar ultraviolet radiation. In the troposphere, ozone acts as a greenhouse gas and near the surface as a toxic pollutant (e.g. Ramaswamy et al. (2001), WHO (2003)). Because the stratosphere can be regarded as a reservoir of ozone, changes in stratosphere-to-troposphere transport (STT) play a very important role in determining the evolution of tropospheric ozone (Zeng and Pyle (2003), Collins (2003), Sudo et al. (2003), Zeng et al. (2010)). The future evolution of tropospheric ozone concentrations remains highly uncertain. A significant part of the uncertainty is due to the climate change scenario, in particular the projected changes in ozone precursor emissions (Stevenson et al. (2013)). Specifically, the global burden of tropospheric ozone ~~is~~ has been estimated to decrease in the RCP6.0 scenario of the Intergovernmental Panel on Climate Change (IPCC) (Sekiya and Sudo (2014), Revell et al. (2015)), and is expected to increase in the RCP8.5 scenario (Banerjee et al. (2016); Meul et al. (2018)) over the 21st century. There are also significant uncertainties for a specific future scenario due to differences between models (Dhomse et al. (2018), Morgenstern et al. (2018)).

Although there is a large uncertainty related to the evolution of chemical precursors of ozone (e.g. WMO (2018)), changes in STT are expected to make an important contribution to future tropospheric ozone changes (e.g. Hegglin and Shepherd (2009), Kawase et al. (2011)). The 2018 WMO Ozone Assessment reports that models project future increases in STT of ozone, but the magnitude of the change is strongly scenario-dependent, and there is no multi-model study to date (Karpechko et al. (2018)). The enhancement of STT is generally attributed to the acceleration of the Brewer-Dobson circulation (BDC) which is predicted consistently by climate model simulations in response to increasing greenhouse gases (Butchart and Scaife (2001)). This enhanced circulation leads to stronger downwelling, and thus to accumulation of ozone in the extratropical lowermost stratosphere, often referred to as the "middle world", thereby increasing the ozone reservoir available for transport into the troposphere. Two branches of the BDC are usually considered, the deep branch with downwelling ~~confined to polar latitudes (poleward of ~60N/S)~~ over polar latitudes and the shallow branch with downwelling over subtropics and ~~midlatitudes~~ middle latitudes (Birner and Bönisch (2011)).

The amount of stratospheric tracer (e.g. ozone) transported into the troposphere will depend on the frequency of cross-tropopause irreversible transport events as well as on the concentration in the lower stratosphere reservoir (Albers et al. (2017)). The latter is controlled by changes in the BDC, in addition to chemical production and loss in the "middle world". ~~The~~ In the subtropics, cross-tropopause irreversible transport occurs typically through isentropic mixing ~~around mid-latitude disturbances in the Atlantic and Pacific storm tracks, and some times associated with tropopause folds (e.g. Stohl et al. (2003)). Therefore, STT is frequently caused by Rossby wave breaking near the tropopause (~~near the subtropical jets (Waugh and Polvani (2000), Yang et al. (2016)). In the extratropics, three dimensional tropopause folds near the polar fronts are eroded or mixed cross-isentropically by turbulent or diabatic processes (Shapiro (1980), Langford and Reid (1998), Sprenger et al. (2003), Stohl et al. (2003), Wernli and Spreng Different methodologies to identify STT can lead to quantitative differences in the net fluxes (e.g. Škerlak et al. (2014), Boothe and Homeyer (2017)~~, Yang et al. (2016)~~). In this paper we ~~will address~~ use idealized tracers with stratospheric sources implemented in the models to evaluate long-term changes in net STT. In addition, we examine the transport mechanisms lead-

ing to the STT increases from the Transformed Eulerian Mean (TEM) perspective. This methodology provides novel insights into the STT mechanisms and their future changes, as it allows evaluating the ~~contributions to the net transport from~~ advective transport by the mean meridional circulation~~and~~, in addition to two-way ~~mixing. In addition, by using idealized tracers with stratospheric sources implemented in the models, we are able to evaluate long-term changes in net STT without having to estimate the flux indirectly from the budget in the "middle word"~~mixing.

Previous studies have obtained estimates of ~~the~~ future changes in STT. Butchart and Scaife (2001) estimate an increase in STT of about 3%/decade, and highlight the important consequences on the rate of chlorofluorocarbon (CFC) removal from the stratosphere. Based on correlations over the observational period between the residual circulation and mid-tropospheric ozone, Neu et al. (2014) estimate an increase in zonal-mean tropospheric ozone concentrations of 2% by the end of the 21st century due to an enhanced BDC. Hegglin and Shepherd (2009) estimate the change in ozone STT flux and obtain a 23% increase from 1965 to 2095 due to climate change in a chemistry-climate model forced with A1B emissions scenario (Nakicenovic et al. (2000)). More recent modeling studies have used artificial tracers to extract the changes due to STT from those due to tropospheric chemistry. Using a stratospheric ozone tracer with no chemical ozone production in the troposphere, O_3S, Banerjee et al. (2016) and Meul et al. (2018) provide the latest estimates of the future increases in the STT of ozone. In particular, Meul et al. (2018) argue that ozone STT flux will increase more than 50% by 2100 under an RCP8.5 scenario.

In the present study we examine future trends in STT from a multi-model perspective using a subset of the CCMI models that provide the necessary output. Section 2 presents the models and tracer output used, Section 3 shows the 21st century trends in the tracers and Section 4 examines the associated changes in transport mechanisms. Section 5 compares the results for two IPCC scenarios, RCP6.0 and RCP8.5, and examines the separate contributions to the STT trends from greenhouse gases (GHG) and ozone-depleting substances (ODS). Section 6 summarizes the main conclusions of the study.

2 Data and Method

We use model output from the CCMI project for seven models over the period 2000-2100. Specifically, we use the REF-C2 simulations as the control, which have time-varying emissions that follow the RCP6.0 IPCC scenario. In Section 5 we use additional sensitivity simulations, including the SEN-C2-RCP85, using the RCP8.5 IPCC scenario, and also SEN-C2-fODS and SEN-C2-fGHG simulations. The last two sensitivity simulations are exactly the same as the REF-C2 simulations, but ozone-depleting substances (ODS) or greenhouse gases (GHG) are fixed to 1960 levels, respectively. This allows attribution of the trends observed in REF-C2 to either external forcing. Morgenstern et al. (2017) provides a description of the CCMI models and simulations, as well as the references for each model. Our analyses are focused on the use of the idealized tracers O_3S, st80 and e90, which are described in Eyring et al. (2013). O_3S is the same as O_3 in the stratosphere and it decays chemically in the troposphere, but it is not produced in this layer. The tracer st80 is continuously set to a specified constant mixing ratio everywhere at 80 hPa and above. Outside this region it is a passive tracer, and in the troposphere it decays with a 25 day e-folding timescale. In addition to these stratospheric tracers, the tropospheric tracer e90 is used. This tracer is emitted throughout the surface (constant mixing ratio boundary condition) and decays everywhere in the atmosphere with a 90-day lifetime. Table 1

[H]

Table 1. Table 1. Available tracer model output for the REF-C2 simulations. ✓ available, ✗ not available, ✳ implementation issues.

	ACCESS	CMAM	EMAC-L47MA	EMAC-L90MA	GEOSCCM	NIWA	WACCM
O_3	✓	✓	✓	✓	✓	✓	✓
O_3S	✓	✓	✓	✓	✓	✓	✓
st80	✳	✓	✳	✳	✓	✳	✓
e90	✗	✓	✗	✗	✓	✗	✓

lists the model output used in this study, including the available tracer fields. Orbe et al. (2018) examined tropospheric transport using some of these tracers, and reported some implementation issues, which are included in Table 1. For instance, in the EMAC model the st80 tracer decays everywhere below 80 hPa, instead of only in the troposphere. For ACCESS and NIWA no known issues have been detected in the implementation of st80 but, as will be shown below, the behavior of the idealized tracer is inconsistent with changes in transport and in O_3S. As will be seen below, the magnitude of O_3S and the fraction of ozone in the troposphere that was accounted for by O_3S varies considerably between models. All models implemented O_3S similarly, with O_3S loss in the troposphere defined as the photochemical loss of ozone including the effects of dry deposition. However the details of which chemical reactions were defined as contributing to photochemical ozone loss, as opposed to recycling, varied between models and explains part of the spread in the magnitude of O_3S. As our primary interest is understanding the long-term trends in O_3S and trends in the contribution of O_3S to tropospheric ozone, we do not further consider the differences in the magnitude of O_3S across the models. Note that the NIWA and ACCESS models have the same atmospheric model, but ACCESS has prescribed ocean from CMIP5 HadGEM2-ES while NIWA has an interactive ocean (Morgenstern et al. (2017)). In addition, we note that the coupled ocean version of EMAC-L47MA is used here, while the EMAC-L90MA simulation has prescribed sea surface temperatures. The SEN-C2-RCP8.5 simulations are only available for CMAM, EMAC-L47MA and WACCM, while the SEN-C2-fODS and SEN-C2-fGHG are available for ACCESS, CMAM, NIWA and WACCM.

The transport changes underlying the changes in stratospheric tracer concentration in the troposphere will be examined through the analysis of the TEM budget. The TEM tracer continuity equation can be written for the zonal mean tracer mixing ratio $\bar{\chi}$ on pressure levels as (Andrews et al. 1987)

$$\bar{\chi}_t = -\bar{v}^*\bar{\chi}_y - \bar{w}^*\bar{\chi}_z + \nabla\cdot\boldsymbol{M} + \bar{P} - \bar{L} + \bar{X} \tag{1}$$

where $\boldsymbol{M} = -e^{-z/H}\left(\overline{v'\chi'} - \frac{\overline{v'T'}}{S}\bar{\chi}_z, \overline{w'\chi'} + \frac{\overline{v'T'}}{S}\bar{\chi}_y\right)$ is the eddy tracer flux vector. The subscripts indicate partial derivatives, $(\bar{v}^*, \bar{w}^*)$ are the residual circulation components, overbars indicate zonal mean and primes deviations from it, $S = HN^2/R$, with the scale height $H = 7$ km and R is the ideal gas constant, and the log-pressure altitude is $z = Hln(p_0/p)$, with $p_0 = 1000$ hPa. The chemical net tendency is given by the production minus loss term, $\bar{P} - \bar{L}$. The resolved transport terms describe advection by the residual circulation, $-\bar{v}^*\bar{\chi}_y - \bar{w}^*\bar{\chi}_z$, and eddy transport, $\nabla\cdot\boldsymbol{M}$, related to two-way mixing. In addition

to these resolved terms there is unresolved or subgrid scale transport, which includes numerical diffusion and parameterized processes such as gravity waves and convection ($\bar{X}$). However, here we will focus on the main resolved transport terms, and we refer the reader to Abalos et al. (2017) for a detailed discussion of the other terms in the budget in WACCM. We note that daily mean data is needed to compute the TEM terms, for both the dynamical and chemical fields. This is not available in all models for the artificial tracers, so we only present the TEM budgets for which daily output was available.

3 Robust increase in future STT

3.1 Timeseries of tracer concentrations

Figure 1 shows timeseries over the 21st century of tropospheric columns of ozone (Fig. 1a), stratospheric ozone O_3S (Fig. 1b) and the artificial tracer st80 (Fig. 1c), as well as the ratio of stratospheric to total ozone O_3S/O_3 (Fig. 1d) for the REF-C2 simulations. The tropospheric tracer columns are based on the thermal tropopause, which is provided as an output for every model. Overall, this figure demonstrates that the concentration of stratospheric tracers in the troposphere will increase in the future, and this result is robust across the CCMI models. The total ozone concentration in the troposphere (Fig. 1a) increases in most models until the middle of the century, and then decreases (except ACCESS and NIWA which show a near constant decrease throughout the century). Comparing the total ozone to the stratospheric ozone evolution (Figs. 1a and 1b) it is clear that the future evolution of chemical production in the troposphere is crucial for the future ozone concentrations. Although not shown here, we have confirmed that a sensitivity WACCM simulation with fixed tropospheric ozone precursor emissions (SEN-C2-fEmis) does not show a decrease in the second half of the century as that seen in Fig. 1a. In the IPCC scenario RCP6.0 under consideration, methane emissions increase until 2080 and then decrease, and nitrogen monoxide emissions decrease since 2000 and more rapidly in the second half of the century (not shown, see Meinshausen et al. (2011)~~and IPCC report 2013~~). The evolution of these gases is likely contributing to the tropospheric ozone column behavior in Fig. 1a. In contrast, Fig. 1b shows that stratospheric ozone (O_3S) in the troposphere increases monotonically thoroughout the century, with a slight reduction of the concentrations over the two last decades in most models. This small reduction is linked to photochemical production of ozone from methane in the stratosphere, as we have confirmed examining additional sensitivity runs of the model CMAM with methane emissions fixed to 1960 levels (not shown). The fraction of stratospheric to total ozone in the troposphere increases linearly in all models (Fig. 1d). In this sense, the models show a good qualitative agreement, although the ratio shows a large spread, from 22 to 45% for the year 2000. Trends in the ratio range from 0.32 to 0.99 %/decade among the models, with CMAM showing the largest trends and GEOSCCM the smallest. Note that the O_3S increase is also seen in ACCESS and NIWA, which combined with the near flat trends in O_3, implies an increase in the stratospheric ozone fraction.

For st80 (Fig. 1c) the timeseries shown are standardized anomalies, i.e. the climatology is subtracted and the result is divided by the year-to-year standard deviation of the full timeseries, in order to focus the attention on the temporal evolution and not on the different magnitude of the concentration across the models. For instance, the magnitude of this artificial tracer in the EMAC models is notably smaller than in the rest (about 50 times), due to an implementation issue (see Section 2). However,

the standardized anomalies show comparable values in Fig. 1c. The artificial tracer st80 shows an increase over the 21st century in all models except for NIWA and ACCESS. The evolution of st80 is very different in each of these two outliers, and cannot be reconciled with the increase seen in O_3S in both models. For this reason in the rest of the paper the st80 tracer will not be considered in these two models. As mentioned above, these two are essentially the same model. We emphasize here that st80 allows directly attributing this increase to enhanced STT, excluding the contribution of changes in stratospheric ozone chemistry present in O_3S. Specifically, an increase in stratospheric ozone is expected from stratospheric cooling and the continued decrease in halogens over the 21st century. ~~For instance,~~ Note that the flattening of O_3S timeseries towards the end of the 21st century linked to the evolution of methane in this scenario is not seen in st80.

Figures 2a and 2~~b~~ c show the trends in ~~O_3S and~~ st80 and O_3S tropospheric columns as a function of the climate response of each model, estimated as the rate of warming of the tropical upper troposphere (30S-30N, 400-150 hPa) under the RCP6.0 scenario. Note that we avoid using the term climate sensitivity because these simulations include several forcings in addition to CO_2, including, for example, time-varying ozone depleting substances (ODS). EMAC-L47MA (coupled ocean), GEOSCCM and WACCM have the smallest climate responses; EMAC-L90MA (prescribed ocean) and CMAM the largest. Although there is some spread, a relation between the two variables can be observed: models with larger climate response tend to produce larger trends in STT, and this relation is more clearly seen for st80 than for O_3S. Note that st80 trends are computed for the standardized timeseries, as shown in Fig. 1. The statistical significance of all trends in the paper is computed with a ~~two-tails~~ two-tail Student t test for the slope at the 95% confidence level (Storch and Zwiers (1999)).

~~Abalos et al. (2017) showed a~~ Given the strong coupling between ~~changes in upper troposphere and lower stratosphere (UTLS) transport and changes in tropopause height. The tropopause is expected to rise in a warming climate due to thermodynamical processes (Vallis et al. (2015)). An important role of the tropopause rise for the BDC trends has been also pointed out recently by Oberländer-Hayn et al. (2016). Figure 2e shows a positive correlation between the change in global mean tropopause altitude and the climate response across the models. This means that models with higher climate response have larger tropopause height rises. Based on these findings, we may~~ tropical upper tropospheric temperature and tropical upwelling, we can hypothesize that the ~~tropopause changes act~~ BDC acts as a mediator between the climate response and STT~~trends. However, Figures 2c~~ , Figures 2b and 2d ~~show that the correlations between STT and tropopause rise are weaker than those between STT and climate response, implying that the relation is not simple~~demonstrate this connection: models with stronger BDC acceleration produce stronger increases in STT for both stratospheric tracers. The transport mechanisms behind these correlations are discussed in the following sections. Overall we argue, based on the spatial structure of the tracer trends and TEM analyses, that zonal mean advective transport by the residual circulation plays an important role in driving STT trends.

In addition to the stratospheric tracers considered above, the evolution of a tropospheric artificial tracer provides a complementary view of the trends in stratosphere-troposphere exchange (STE). Figure ~~??~~ 2e shows trends in the tropospheric tracer e90 in the troposphere for the three models that provide this output (CMAM, GEOSCCM and WACCM). The magnitude of the tracer trends increases with the climate response of the model. Note that there is a non-significant trend in WACCM, different from Figure 13 in Abalos et al. (2017), which showed a significant decrease of the e90 concentrations averaged over the troposphere (in ppbv). However we note that the difference in the trends in the tropospheric average in Abalos et al. (2017)

versus those in the tropospheric column in Fig. ~~??a~~ 2c is not significant, since the 95% confidence intervals overlap between the two. The other two models show a significant net decrease, larger for CMAM. ~~This~~ The reduction of tropospheric tracer concentrations in the troposphere is consistent with a more efficient transport into the stratosphere, ~~and is related primarily~~ which is indeed related with stronger tropical upwelling in the future~~(~~, as shown in Fig. 2f (see also e.g. Rind et al. (2001), Abalos et al. (2017)).

3.2 Spatial structure of the tracer trends

As a first step to understand the changes in transport processes leading to long-term trends in the STT rates seen in Figs. 1 ~~-??~~and 2, in this Section we examine the zonal mean spatial structure of the trends. We note that the trends in EMAC-L90MA are qualitatively very similar to those in EMAC-L47MA and thus only the latter is shown in the rest of the paper, denoted EMAC.

Starting with the tropospheric tracer, Figure 3 shows the spatial structure of the trends in e90. The three models yield highly consistent results, and the magnitude scales with the climate response shown in Fig. ~~??~~2e. Using the TEM formalism, Abalos et al. (2017) examined the causes leading to these trend patterns~~. In the stratosphere, the~~ , showing that they reflect known effects of climate change. The increase in the ~~tropics~~ tropical lower stratosphere is attributed to enhanced BDC tropical upwelling, while the ~~increase near the extratropical tropopause is due~~ increases in the extratropical UTLS are at least partly linked to enhanced isentropic mixing in this region. The rise of the tropopause ~~altitude~~ with climate change plays a key role in these ~~stratospheric changes, shifting upward the region~~ changes, as it implies an upward shift of the regions of wave dissipation, and ~~thus isentropic mixing and~~ therefore an upward shift of the residual circulation wave forcing (Oberländer-Hayn et al. (2016)) and of isentropic mixing (Abalos et al. (2017)). In addition, as the troposphere expands, the composition of the UTLS becomes more tropospheric-like, since tracers encounter the change in transport regime defined by the tropopause at higher levels. In the extratropical troposphere, the negative trends are associated with weaker meridional mass circulation and isentropic mixing. In the tropical troposphere, they are ~~due to enhanced~~ consistent with more intense and deeper circulation in the upper part of the Hadley cell, linked to enhanced deep convection and connected to the stronger BDC tropical upwelling. In simple terms, the reduction in the tropospheric e90 concentrations reflects a less efficient transport from the surface into the extratropical free troposphere, and a more efficient troposphere-to-stratosphere transport in the future.

The trends in O_3S are shown in Figure 4. In the stratosphere, ozone decreases in the tropics and increases in the extratropics, and this pattern is expected from the acceleration of the residual circulation seen in all models (as will be shown below). There is an interhemispheric asymmetry in the lowermost stratosphere, with stronger positive trends in the SH extending to lower levels than in the NH. Only in two models, EMAC and GEOSCCM, there are positive trends around the NH extratropical tropopause. This is probably due to the cancellation of the effects of GHG and ODS in these two models, as will be argued in Section 5. The large SH O_3S positive trends are due to the recovery of the Antarctic ozone hole. In contrast, the negative trends around the NH extratropical tropopause are consistent with trends in the artificial tracer e90 identified in Fig. 3 (in both hemispheres). As stated above, these trends around the extratropical ~~tropopause are attributed to changes in isentropic mixing in this region, and~~ UTLS constitute a fingerprint of the tropopause rise~~(see Abalos et al. (2017))~~. This is confirmed by looking

at the O_3S trends in tropopause-relative coordinates, in which the band of negative trends ~~at~~ around the NH tropopause is not present (not shown). The change in tropopause altitude as a function of latitude over the 21st century is shown in Figs. 3, 4 and 5. In the troposphere, O_3S trends are positive, and their spatial structure reveals a common pattern across models (Fig. 4). The largest trends are found in the subtropics, near 30N/S in the middle to upper troposphere (∼500-200 hPa). The positive trends extend to higher latitudes below the tropopause, and these extratropical increases are stronger in the SH than in the NH in all models. The deep tropics display a local minimum and near zero trends or even negative are found next to the ground in the tropics, consistent with little influence of stratospheric air in these regions. This pattern is consistent with those shown by Banerjee et al. (2016) and Meul et al. (2018) in individual models.

In Figure 5 we use the artificial tracer st80 in order to examine the trend patterns for an artificial tracer with constant and homogeneous stratospheric sources. Note that this tracer is only useful in the troposphere, since it has a constant fixed value of 200 ppbv at and above 80 hPa, and thus the stratospheric values are not shown. The st80 trends in EMAC (Fig. 5b) have been multiplied by an arbitrary factor of 50 in order to fit the scale due to a known implementation issue (see Section 2). The st80 trends in Fig. 5 show more hemispherically symmetric patterns as compared to Fig. 4, with negative trends near the extratropical tropopause in both hemispheres (except in EMAC), as seen in the NH trends for O_3S and consistent with e90 trends in Fig. 3. In addition, there are positive trends maximizing in the subtropical troposphere in both hemispheres, that extend to higher latitudes below the region of negative trends linked to the extratropical tropopause. This structure is similar to that seen for O_3S, although not exactly comparable due to differences in the gradients between these two tracers and their different stratospheric source distributions ~~.~~ (see climatology contours in Figs. 4 and 5).

In the deep tropical upper troposphere all models show a local minimum, although CMAM and EMAC show higher concentrations at the equator than GEOSCCM and WACCM. ~~The~~ Note that the former models also show higher climatological st80 concentrations in the deep tropics~~are likely linked to the altitude of the tropopause in the models. In particular CMAM shows the highest tropopause, with the tropical tropopause altitude close to the 80 hPa level in which st80 has its constant source (Fig. 5a)~~, suggesting leakier tropical tropopauses in these models. As the tropopause rises in the simulated future climate ~~, this can result in enhanced vertical diffusion~~ it gets closer to the source level of st80 (80 hPa), and vertical transport into the tropical troposphere ~~.~~ is enhanced. This effect is magnified in models with a higher tropopause, such as CMAM (Fig. 5a).

Overall, the O_3S and st80 trend patterns highlight common features in all models, and in the next section we investigate the transport changes that lead to these trends in the stratospheric tracers.

4 Trends in TEM transport terms

To facilitate interpretation of the TEM transport terms that will be shown next, Figure 6 shows the trends in the residual circulation streamfunction for the various models included in this study. In the stratosphere, all models show an acceleration of the BDC in both hemispheres. However, while in the NH the acceleration extends from the tropics to polar latitudes, in the SH there is a cell of opposite sign at high latitudes. This is due to the impact of the ozone hole recovery on the residual circulation. Specifically, the ozone recovery weakens the downwelling in the SH high latitudes over the 21st century, reversing the acceler-

ation induced during the ozone hole formation over the ~~las~~ last decades of the 20th century (Polvani et al. (2018), Abalos et al. (2019)). This behavior is observed in most CCMI models (Morgenstern et al. (2018), ~~Polvani et al. 2019~~Polvani et al. (2019)). Figure 6 confirms this common behavior, with EMAC being an exception with near zero residual circulation trends in the SH polar latitudes. The fact that this feature does not appear as clearly in this model could be linked to a weak SH polar vortex.

In the troposphere, most models show a deceleration of the residual circulation in the extratropics of both hemispheres. In the tropics, all models show a strengthening of the upper part of the Hadley cell, just below the acceleration of the shallow branch of the stratospheric circulation. As shown in Abalos et al. (2017), this strengthening is closely linked to the upward shift of the tropopause. As will be shown below, the enhanced downwelling of the Hadley cell in the upper subtropical troposphere cooperates with the enhanced shallow branch of the BDC to enhance advective downward transport of the stratospheric tracers into the troposphere. This leads to the subtropical upper tropospheric maxima in the O_3S and st80 trend patterns seen in Figs. 4 and 5. Moreover, Figure 6 demonstrates that this mechanism is present in all models.

Figures 7 and 8 show the 21st century change in the advective transport term for the tracers O_3S and st80, respectively, in four models (CMAM, EMAC, GEOSCCM and WACCM). We note that the daily output for CMAM was obtained three times per month, while the other models had output for every day of the year. In order to increase the amount of data in CMAM, we considered differences between the first and last half of the century for this model. For the others, differences between the first and last 10 years of the century are considered.

The O_3S advective term (Fig. 7) shows a decrease ~~in~~ of the concentrations in the tropical lower stratosphere due to enhanced upwelling, and increases at extratropical latitudes due to enhanced downwelling~~in the deep branch of the BDC. While in the NH the extratropical increases extend into polar latitudes , in the polar SH there are negative ozone trends by advection above 20 km in all models except EMAC. This is due to the impact of ozone recovery on the residual circulation highlighted above, with downwelling weakening over the 21st century in this region (shown~~ . At polar latitudes in the SH we see the effects of ozone hole recovery, which are twofold: an increase of O_3S concentrations in the polar lower stratosphere, and a weakening of the residual circulation polar downwelling (seen in Fig. 6~~). Interestingly, in the SH polar lower stratosphere below~~ ; see also Polvani et al. (2018)). The latter dominates above ~20 km, resulting in negative trends in advection of O_3S. Below 20 km, the ozone recovery due to decreasing ODS ~~concentrations compensates this reduction in downwelling~~dominates, and the net effect is ~~to increase the~~ an increase in ozone downward transport~~in that region~~. As a result, there is enhanced advective ~~transport~~ STT of stratospheric ozone ~~into the troposphere~~ at polar latitudes in both hemispheres~~. In addition, all~~ , due to a larger reservoir in the lowermost stratosphere (and not to stronger downwelling across the tropopause, see Fig. 6). In the NH, the enlarged lower stratospheric ozone reservoir is partly due to the acceleration of the deep branch of the BDC (Fig. 7). In the SH, where the BDC actually decelerates, it is exclusively due to reduced photochemical destruction as ODS concentrations decline.

All models show positive trends in ozone due to advection near the subtropical tropopause (approximately 30N and 30S at 150 hPa). The arrows indicate an enhancement of the amount of stratospheric ozone being advected across the tropopause into the troposphere in these regions by the enhanced shallow branch of the BDC and top of the Hadley cells. These patterns lead

to the subtropical tongues observed in the O_3S trends in Fig. 4. Hence, both shallow and deep branches of the BDC lead to enhanced stratospheric ozone transport into the troposphere.

Figure 8 shows the advective transport term for the artificial tracer st80 in the same four models. Again, all models show consistent features. In particular, similar to the behavior seen in O_3S, there is enhanced downward transport into the troposphere in the subtropics linked to the shallow BDC and top of the Hadley cell. These patterns lead to the subtropical tongues in the st80 trends seen in Fig. 5. Note that the tongue structure is somewhat different in the two tracers, due to the different background gradients (compare the climatological concentrations in Figs. 4 and 5). At polar latitudes ~~only~~ in the NH, GEOSCCM and WACCM show enhanced downward transport into the troposphere~~in the NH hemisphere~~. This is ~~due to~~ consistent with lower stratospheric reservoir enlargement of st80 by the enhanced downwelling of the deep branch, as seen for O_3S. The fact that CMAM and EMAC-L47MA fail to capture these trends ~~for st80 while showing them for O_3S suggests that there might be~~ reflects issues with the st80 idealized tracer concentrations in the stratosphere (~~this is indeed the case for EMAC, see Table 1).~~ see Orbe et al. (2018), supplementary material Fig. S2). In particular, these two models do not show an increase in st80 concentrations in the NH lower stratosphere, as would be expected from the strengthened BDC. On the other hand, the fact that none of the models show enhanced downward transport of st80 at SH polar latitudes confirms that the ~~enhanced~~ enlarged O_3S ~~transport~~ reservoir and subsequent enhanced STT in this region seen in Fig. 7 is exclusively linked to ozone recovery.

While we find good correspondence among models in the advective transport term (Figs. 7 and 8), the eddy mixing term is subject to larger uncertainties and there is a larger spread among models. This term is computed from meridional and vertical tracer eddy fluxes (see Eq. 1 and related discussion) which are highly sensitive to numerical errors arising from different sources including limited temporal resolution of the output, implicit diffusion in the model transport scheme and vertical interpolations (see Abalos et al. (2017) for a discussion of these errors in WACCM). Since understanding in detail the sources of uncertainty in each model is beyond the scope of the study and our goal is to extract robust trend features in the transport terms, we only include results for models showing consistent behavior. At the same time, we warn that the conclusions extracted for the eddy term should be considered more uncertain than those found for the advective term, given the limited inter-model agreement.

Figure 9 shows the trends in the eddy term for O_3S (a and b) in CMAM and WACCM and for st80 in GEOSCCM and WACCM (c and d). In the stratosphere there is enhanced isentropic mixing transporting O_3S from high latitudes into the tropics in both models, and enhanced eddy transport out of the SH polar stratosphere. Of greater interest for this study are the trends in cross-tropopause transport. For both tracers there is enhanced isentropic mixing across the extratropical tropopause, which leads to increases in ozone concentrations in the upper troposphere middle latitudes in both hemispheres (30-60N/S). In addition to increasing the tropospheric concentrations, this enhanced eddy transport decreases the tracer concentrations in the lowermost extratropical stratosphere. This is consistent with the enhanced isentropic eddy transport in e90 found by Abalos et al. (2017) leading to the increased concentrations in this tracer around the extratropical tropopause (Fig. 3). Hence, the same mechanism ~~leads~~ likely contributes to the negative trends in st80 and $O3S$ (only in the NH) around the extratropical tropopause (Figs. 4 and 5). This is added to the direct effect of the tropospheric expansion on the extratropical UTLS composition, as mentioned in Section 3.2.

Finally, there is enhanced cross-tropopause near-vertical transport of st80 in the tropics, which contributes to enhance the concentrations in the tropical upper troposphere on both sides of the equator. This feature is mainly due to the fixed st80 concentrations above 80 hPa: as the tropical tropopause rises and gets close to this level, vertical gradients strengthen and lead to cross-tropopause transport.

~~Overall~~Note that we do not attempt to provide a quantitative estimate of the contribution from each transport term to the net tracer trends. The total balance should include additional transport terms such as convection, diffusion, and transport by subgrid-scale waves, as well as the chemical tendency term (important for O_3S). Even if those terms were considered the budget would not be exactly closed, due to the numerical issues such as those listed in Abalos et al. (2017), which are model-dependent. Nevertheless, the two resolved transport terms provide valuable information on the different effects of these transport mechanisms on the tracer trends. Specifically, Figures 7 to 9 suggest that the trend patterns seen in O_3S and st80, ~~specifically the subtropical tongues, are largely explained by the~~ particularly in the subtropics and at polar latitudes, result from enhanced advective transport into the troposphere~~, and not by changes in two-way mixing~~. The relevance of the mean ~~advective circulation~~ advection by the stratospheric residual circulation and the upper part of the Hadley cell for the STT trends is a novel result that has not been considered before.

5 Dependence on emission scenario

These results shown up to now apply for the RCP6.0 scenario of the IPCC but, as mentioned in the Introduction, other scenarios may lead to different results. Figure 10 shows timeseries of tropospheric columns of various stratospheric tracers over the 21st century ~~as in Fig. 1 but for~~ comparing the RCP6.0 to the RCP8.5 ~~scenario~~scenarios. This data is only available in three models: CMAM, EMAC-L47MA and WACCM. ~~Comparing Fig. 10a to Fig. 1a~~ Figure 10a reveals a clear difference in the evolution of ozone in the troposphere, which increases throughout the century in the RCP8.5 scenario in the three models and decreases in the RCP6.0 scenario. Part of ~~the difference in~~ this difference in the evolution of ozone could be explained by differences in the precursor emissions between the two scenarios. Methane increases monotonically throughout the century in the RCP8.5 scenario, while in the RCP6.0 scenario it increases at a much slower rate and then it decreases during the last two decades of the century (Meinshausen et al. (2011)). ~~These differences in precursor (methane) emissions could explain the different ozone trends between the two scenarios.~~ In contrast, nitrogen monoxide emissions decrease over the 21st century in the two scenarios, with similar slopes (not shown), so they cannot explain the differences. In addition to these chemical effects, the ~~strong~~ stronger acceleration of the BDC in the more extreme scenario leads to enhanced ozone STT as compared to the other scenario. ~~Hence, we suggest~~ The connections established above between the BDC acceleration and STT suggest that this dynamical effect is important. Finally, there could be a contribution from the faster rate of stratospheric ozone recovery due to larger stratospheric cooling in RCP8.5 (WMO (2018)). Overall, we argue that both chemical and dynamical effects ~~are contributing to the faster~~ contribute to the fast increase in tropospheric ozone in RCP8.5, absent in RCP6.0.

Consistent with a ~~stronger~~ larger increase in ozone STT, O_3S increases faster in the more extreme scenario (Fig. 10b). ~~A clear~~ The largest difference between the two scenarios for this tracer is seen in the last 20 years of the simulations, where

O_3S concentrations remain flat in RCP6.0 but continue to increase in ~~the~~ RCP8.5~~scenario~~. As mentioned in Section 3.1, this flattening of O_3S in RCP6.0 is related to reduced ozone production from methane in the lower stratosphere. ~~We note that this effect also likely contributes to the faster increase in O_3S in RCP8.5 especially in the first half of the century, when the differences in BDC strength between the two scenarios are not as large (not shown). Finally, there could be a contribution from the different rate of stratospheric ozone recovery due to larger stratospheric cooling in RCP8.5 (WMO (2018)). The~~ There is no significant difference in the ratio of stratospheric to total ozone between the two scenarios (Fig. 10d)~~also increases faster in this extreme scenario than in the RCP6.0~~. For st80 (Fig. 10c) there is a steady increase in the RCP8.5 for all models, larger than in the RCP6.0 scenario. In CMAM and EMAC-L47MA this increase is enhanced over the last 20 years, perhaps due to the tropical tropopause being close to 80 hPa by the end of the century. The 21st century trends in O_3S and st80 in the two scenarios are compared in Figs. 10e and 10f. In all models the climate response is stronger in the higher emissions scenario~~. The tracer trends in general are significantly stronger in the RCP8.5 scenario~~, and the tracer trends are significantly (2-3 times) stronger, consistent with more severe climate change and associated transport changes. ~~An exception is found for st80 in CMAM, which shows statistically undistinguishable trends in both scenarios. This could be linked to the tropical tropopause being at nearly 80 hPa in this model for both scenarios by the end of the century.~~

Polvani et al. (2018) showed that the future acceleration of the BDC due to the increase in GHG is partly compensated by the decrease in ozone-depleting substances (ODS). More specifically they showed that the global mean age of air trends in the 21st century are reduced by about half with respect to those observed over the last few decades of the 20th century. The main reason for this decrease is the weakening of the polar SH downwelling associated with the recovery of the ozone hole. Here, we examine the separate contributions to the STT trends from changes in the GHG and ODS emissions. Banerjee et al. (2016) and Meul et al. (2018) examined the impact of these two forcings on ozone transport into the troposphere in individual models, and found that increases in GHG lead to increases in stratospheric ozone in the subtropics, while ozone recovery leads to ozone enhancement at higher latitudes.

Figure 11 shows the trends in O_3S for the three models that output this tracer (ACCESS, CMAM and NIWA) for sensitivity simulations with concentrations of ODS or GHG fixed to 1960 levels. Since we are looking at trends for the 21st century, the fixed-ODS simulations can be conceptualized as characterizing the impact of the increase of GHG through the century, and the fixed-GHG simulations as characterizing the impact of the elimination of halogens. Comparing Figs. 11a 11c and 11e with Fig. 4 it is clear that increases in stratospheric ozone in the troposphere are more modest when ODS concentrations are fixed. This ~~simply~~ reflects the fact that stratospheric ozone recovery leads to more ozone being transported into the troposphere. In agreement with previous studies, in the fixed-ODS simulations the O_3S increases are limited to the subtropical region. The negative trends near the extratropical tropopause are consistent with the changes ~~in mixing~~ associated with the tropopause rise in response to climate change mentioned above (Figs. 3-5, Abalos et al. (2017)). It becomes evident now that the band of negative O_3S trends in the NH extratropical UTLS seen in Fig. 4 is due to the effect of GHG increases, while ODS increases yield positive O_3S trends in this region. Consistently, we conclude that in the two models that do not show such band of negative trends, EMAC and GEOSCCM, the stratospheric ozone recovery overwhelms the GHG effect (Figs. 4c and 4d). Note

that we cannot provide exact proof of this conclusion because we do not have fixed ODS and fixed GHG simulations for those two models in particular.

The differences between the control and sensitivity simulations are especially evident in the SH, where the ozone hole is located and thus the ozone recovery effect is the strongest. This effect of ozone recovery is isolated in the fixed-GHG sensitivity simulations (Figs. ~~12b, 12d and 12~~11b, 11d and 11f). These clearly show that increases in stratospheric ozone concentrations result in increased STT mostly in the extratropics. The results in Fig. ~~12~~ 11 are highly consistent with those from previous studies highlighted above (Banerjee et al. (2016) and Meul et al. (2018)).

Analysis of the time series of globally integrated O_3S tropospheric columns for the REF-C2, SEN-C2-fODS and SEN-C2-fGHG simulations reveals that, in ACCESS and NIWA, the increase in $O3S$ STT is dominated by the effect of ozone recovery (not shown). In contrast, in CMAM both GHG and ODS contribute approximately the same to the net trends in $O3S$ STT. Thus, there is no agreement in the relative contributions of these two external forcing to STT increases for $O3S$.

In order to separate the effects of changes in transport from those of stratospheric ozone recovery we now look at st80 trends. Figure 12 shows trends in the sensitivity simulations for st80 in CMAM and WACCM (note that ACCESS and NIWA are not used for the reasons explained in Section 3.1). In contrast with O_3S, the st80 trends in the fixed-ODS runs (Figs. 12a and 12c) are very similar to those in the control simulations for both models not only in the subtropics but also at high latitudes (Fig. 5). This confirms that the changes in transport mechanisms examined in the previous section are mainly caused by the increase in GHG. On the other hand, the trends in the fixed-GHG simulations (Figs. 12b and 12d) are much more uncertain and are statistically insignificant over large regions of the troposphere. For instance, the two models show opposite sign trends in the NH (not significant in WACCM, and also not consistent among 3 different members, not shown). This difference between the O_3S and st80 trends in the fixed-GHG scenario ~~reveals~~ confirms that the trends in O_3S are ~~mostly~~ due to the increase ~~in ozone concentrations~~ of ozone concentrations directly associated with ODS decline through changes in photochemistry, rather than by dynamical changes induced by ~~ozone recovery (or ODS decrease)~~ODS decline. Nevertheless, one consistent feature in the two models is the increase in st80 concentrations in the SH high latitude upper troposphere (Figs. 12b and 12d). This is linked to a small downward shift of the tropopause in these simulations associated with the weakening of polar downwelling, a dynamical effect of the recovery of the Antarctic ozone hole (Polvani et al. (2018), ~~Polvani et al. 2019~~Polvani et al. (2019)). Note that this SH tropopause shift is opposite to that associated with GHG increases (compare the tropopauses in Figs. 12a and 12c to Figs. 12b and 12d). Consistently, the positive st80 trends due to ozone recovery near the SH tropopause partly offset the decrease due to increasing GHG (the net result is still a decrease, as shown in Fig. 5). Besides this specific feature, no robust conclusion can be extracted on future changes in STT if GHG concentrations are fixed. The dominant role of climate change on the st80 STT trends is further confirmed for both models by comparing timeseries for the two fixed-forcing simulations in Fig. 12 to the all-forcing (REF-C2) runs (not shown).

6 Conclusions

In this study we investigated the future trends in stratosphere-troposphere exchange (STE), with a specific focus on stratosphere-to-troposphere transport (STT), using output from various models participating in CCMI in order to extract robust signals. Idealized tracer data provides a unique opportunity to evaluate changes in transport, separated from changes in chemical processes due, for instance, to changes in precursor concentrations. We show that all models agree in predicting an enhancement of the concentrations of stratospheric tracers in the troposphere in the future. The models project a near-linear increase in the fraction of stratospheric to total ozone in the troposphere between 10 and 20% over the 21st century with respect to the 2000-2010 mean values. This increase reflects the combined effects of increased transport - the tropospheric column of stratospheric ozone increases 10-16% - and reduced chemical production in the troposphere during the second half of the 21st century, in the RCP6.0 emission scenario considered here. These results are consistent with previous studies using individual models. Our multi-model approach allows extracting a correlation between the climate response and the magnitude of the STT trends in the different models. ~~As shown in previous studies, tropopause altitude is a key player in the STE trends. While we obtain a positive correlation between tropopause rise in a future climate and climate response across models, a clear connection between tropopause rise and STT trends cannot be established.~~

In addition to ozone and stratospheric ozone (O_3S), we analyze the idealized tracer st80, which is independent of chemistry in the stratosphere as well as in the troposphere. The patterns of trends in O_3S and st80 exhibit common features, revealing the fingerprints in the tracer trends of changes in transport alone~~(~~, excluding changes in stratospheric ozone chemical sources and sinks~~)~~. One of the key features identified in the tracer trends are maximum increases in the subtropical troposphere of both hemispheres. In addition, the positive trends extend to high latitudes in the lower troposphere (below approximately 400 hPa). Negative trends are generally observed around the extratropical tropopause, except for O_3S in the SH, where stratospheric ozone recovery leads to an increase in the concentrations across the tropopause.

Examination of the TEM tracer continuity equation allows evaluation of the changes in transport processes leading to the enhanced STT, separating advective transport by the residual circulation from eddy transport, linked to two-way mixing. We find that enhanced advective transport plays a key role in the subtropical trend maxima for both O_3S and st80. This is linked to the acceleration of the shallow branch of the residual circulation and the strengthening of the top of the Hadley cell. Note that the Hadley cell strengthening does not extend into the lower troposphere (e.g. Fig. 6). This is consistent with recent studies arguing that metrics of the Hadley cell should be considered separately for the upper and lower parts (Davis and Davis (2018), Waugh et al. (2018)).

~~In the extratropics, we find enhanced~~ Enhanced downward advective transport ~~by~~ due to the acceleration of the deep branch of the BDC contributes to STT over polar latitudes in the NH only, by accumulating the tracers in the "middle world" reservoir. In the SH, the dynamical effects of ozone hole recovery prevail and there is a weakening of polar downwelling (Polvani et al. (2018)). Nevertheless, ~~O_3S STT~~ STT of O_3S increases due to the higher ozone concentrations in the lower stratosphere ~~.~~ as ODS decline.

Although larger uncertainties are obtained for the eddy transport term, a consistent feature identified is an enhancement of ~~isentropic eddy transport near the extratropical tropopause. This leads to decreases in stratospheric tracer concentrations in this region and contributes to the increases~~ eddy transport in the extratropical ~~troposphere. Such enhanced mixing around the extratropical tropopause is also~~ UTLS. A similar feature was observed for the ~~idealized~~ tropospheric tracer e90 ~~, and it is linked to an upward shift~~ by Abalos et al. (2017), and was linked to the rise of the extratropical tropopause and associated ~~changes in the wave propagation conditions (Abalos et al. (2017)). We argue that the same mechanism leads~~ upward shift of the region of wave dissipation. These changes in mixing likely contribute to the negative trends in the stratospheric tracers around the extratropical tropopause, in addition to the direct effects of the upward expansion of the troposphere. Certainly, the rise of the tropopause is key to explain these extratropical UTLS trends, which disappear when tropopause-relative coordinates are used.

While the same qualitative results apply when the more extreme scenario RCP8.5 is considered, the tropospheric column of stratospheric ozone increases 40-50% by the end of the 21st century (with respect to the 2000-2010 mean values). This implies an increase more than 3 times larger than in the RCP6.0 scenario. However, this result is limited to two models due to limited availability of output. The results for st80 also suggest a larger increase for the high emission scenario: ~~two out of three models show 1.5~~ the models show 2-3 times larger trends in the RCP8.5 scenario. We also explore the ~~dependence on the future emission scenario and the roles of~~ roles of two key forcings, GHG and ODS, separately. Using O_3S, Banerjee et al. (2016) and Meul et al. (2018) showed that increasing GHG lead to enhanced stratospheric ozone in the subtropical troposphere, while ozone recovery leads to more modest enhancements throghout the extratropics. Here we confirm that this is the case also for all the models providing the specific sensitivity simulations. Moreover, using the idealized tracer st80 we show that the robust STT trends are primarily attributed to increasing GHG emissions. Ozone recovery (or ODS reduction) does not drive consistent trends in STT across models. However, in two out of the three available models, ozone recovery is mainly responsible for the observed increase in ozone STT into the troposphere. This apparent contradiction is simply explained by the fact that such increase in ozone STT is due to stratospheric ozone photochemistry, and not to changes in transport processes. However, these relative roles of GHG and ODS can be different in the more extreme climate change scenario, though this cannot be addressed with the current model output.

The assessment of future STT trends is key for interpreting the future evolution in tropospheric ozone, and the present study demonstrates the usefulness of idealized tracers to better constrain transport changes. At the same time, we emphasize that tropospheric chemistry, and in particular of the evolution of precursor emissions in each scenario, remains a major source of uncertainty.

Author contributions. MA wrote the draft and carried out the analyses. CO and DK contributed with additional simulations. All coauthors contributed with discussions, expertise on the models and comments on the draft.

Competing interests. The authors declare no competing interests.

Acknowledgements. MA acknowledges funding from the Program Atracción de Talento de la Comunidad de Madrid (2016-T2/AMB-1405) and the Spanish National Project STEADY (CGL2017-83198-R). This study has been partly carried out using the high performance computing and storage facilities provided by CISL/NCAR. The EMAC simulations have been performed at the German Climate Computing Centre (DKRZ) through support from the Bundesministerium für Bildung und Forschung (BMBF). DKRZ and its scientific steering committee are gratefully acknowledged for providing the HPC and data archiving resources for the consortial project ESCiMo (Earth System Chemistry integrated Modelling). We acknowledge the UK Met Office for use of the MetUM. This research was supported by the NZ Government's Strategic Science Investment Fund (SSIF) through the NIWA programme CACV. Olaf Morgenstern acknowledges funding by the New Zealand Royal Society Marsden Fund (grant 12-NIW-006). The authors wish to acknowledge the contribution of NeSI high-performance computing facilities to the results of this research. New Zealand's national facilities are provided by the New Zealand eScience Infrastructure (NeSI) and funded jointly by NeSI's collaborator institutions and through the Ministry of Business, Innovation and Employment's Research Infrastructure programme (https://www.nesi.org.nz). The GEOSCCM is supported by the NASA MAP program and the high-performance computing resources were provided by the NASA Center for Climate Simulation (NCCS).

References

Abalos, M., Randel, W. J., Kinnison, D. E., and Garcia, R. R.: Using the artificial tracer e90 to examine present and future UTLS tracer transport in WACCM, Journal of the Atmospheric Sciences, pp. JAS–D–17–0135.1, https://doi.org/10.1175/JAS-D-17-0135.1, http://journals.ametsoc.org/doi/10.1175/JAS-D-17-0135.1, 2017.

Abalos, M., Polvani, L., Calvo, N., Kinnison, D., Ploeger, F., Randel, W., and Solomon, S.: New Insights on the Impact of Ozone-Depleting Substances on the Brewer-Dobson Circulation, Journal of Geophysical Research: Atmospheres, 124, 2435–2451, https://doi.org/10.1029/2018JD029301, http://doi.wiley.com/10.1029/2018JD029301, 2019.

Albers, J. R., Perlwitz, J., Butler, A. H., Birner, T., Kiladis, G. N., Lawrence, Z. D., Manney, G. L., Langford, A. O., and Dias, J.: of Stratosphere-to-Troposphere Ozone Transport, pp. 1–27, 2017.

Banerjee, A., Maycock, A. C., Archibald, A. T., Abraham, N. L., Telford, P., Braesicke, P., and Pyle, J. A.: Drivers of changes in stratospheric and tropospheric ozone between year 2000 and 2100, Atmospheric Chemistry and Physics, 16, 2727–2746, https://doi.org/10.5194/acp-16-2727-2016, http://www.atmos-chem-phys-discuss.net/15/30645/2015/http://www.atmos-chem-phys.net/16/2727/2016/, 2016.

Birner, T. and Bönisch, H.: Residual circulation trajectories and transit times into the extratropical lowermost stratosphere, Atmospheric Chemistry and Physics, 11, 817–827, https://doi.org/10.5194/acp-11-817-2011, 2011.

Boothe, A. C. and Homeyer, C. R.: Global large-scale stratosphere-troposphere exchange in modern reanalyses, Atmospheric Chemistry and Physics, 17, 5537–5559, https://doi.org/10.5194/acp-17-5537-2017, 2017.

Butchart, N. and Scaife, A. A.: Removal of chlorofluorocarbons by increased mass exchange between the stratosphere and troposphere in a changing climate, Nature, 410, 799–802, https://doi.org/10.1038/35071047, 2001.

Collins, W. J.: Effect of stratosphere-troposphere exchange on the future tropospheric ozone trend, Journal of Geophysical Research, 108, 1–10, https://doi.org/10.1029/2002JD002617, 2003.

Davis, N. A. and Davis, S. M.: Reconciling Hadley Cell Expansion Trend Estimates in Reanalyses, Geophysical Research Letters, pp. 439–446, https://doi.org/10.1029/2018GL079593, 2018.

Dhomse, S., Kinnison, D., Chipperfield, M. P., Cionni, I., Hegglin, M., Abraham, N. L., Akiyoshi, H., Archibald, A. T., Bednarz, E. M., Bekki, S., Braesicke, P., Butchart, N., Dameris, M., Deushi, M., Frith, S., Hardiman, S. C., Hassler, B., Horowitz, L. W., Hu, R.-M., Jöckel, P., Josse, B., Kirner, O., Kremser, S., Langematz, U., Lewis, J., Marchand, M., Lin, M., Mancini, E., Marécal, V., Michou, M., Morgenstern, O., O'Connor, F. M., Oman, L., Pitari, G., Plummer, D. A., Pyle, J. A., Revell, L. E., Rozanov, E., Schofield, R., Stenke, A., Stone, K., Sudo, K., Tilmes, S., Visioni, D., Yamashita, Y., and Zeng, G.: Estimates of Ozone Return Dates from Chemistry-Climate Model Initiative Simulations, Atmospheric Chemistry and Physics Discussions, pp. 1–40, https://doi.org/10.5194/acp-2018-87, https://www.atmos-chem-phys-discuss.net/acp-2018-87/, 2018.

Eyring, V., Lamarque, J.-F., Hess, P., Arfeuille, F., Bowman, K., Chipperfield, M. P., Duncan, B., Fiore, A., Gettelman, A., Giorgetta, M. A., Granier, C., Hegglin, M., Kinnison, D., Kunze, M., Langematz, U., Luo, B., Martin, R., Matthes, K., Newman, P. A., Peter, T., Robock, A., Ryerson, T., Saiz-Lopez, A., Salawitch, R., Schultz, M., Shepherd, T. G., Shindell, D., Stähelin, J., Tegtmeier, S., Thomason, L., Tilmes, S., Vernier, J.-P., Waugh, D. W., and Young, P. J.: Overview of IGAC/SPARC Chemistry-Climate Model Initiative (CCMI) Community Simulations in Support of Upcoming Ozone and Climate Assessments, SPARC Newsletter, pp. 48–66, 2013.

Hegglin, M. I. and Shepherd, T. G.: Large climate-induced changes in ultraviolet index and stratosphere-to- troposphere ozone flux, Nature Geoscience, 2, 687–691, https://doi.org/10.1038/ngeo604, http://dx.doi.org/10.1038/ngeo604, 2009.

Karpechko, A., Maycock (Lead Authors), A. C., Abalos, M., Akiyoshi, H., Arblaster, J. M., Garfinkel, C. I., Rosenlof, K. H., Sigmond, M., Aquila, V., Banerjee, A., Chrysanthou, A., Ferreira, D., Garny, H., Gillett, N., Mills, M. J., Randel, W. J., Ray, E., Seviour, W., Swart, N., Editors, R., Cagnazzo, C., and Polvani, L.: Chapter 5: Stratospheric Ozone Changes and Climate, in: Scientific Assessment of Ozone Depletion: 2018, chap. 5, World Meteorological Organization, Geneva, Switzerland, 2018.

Kawase, H., Nagashima, T., Sudo, K., and Nozawa, T.: Future changes in tropospheric ozone under Representative Concentration Pathways (RCPs), Geophysical Research Letters, 38, n/a–n/a, https://doi.org/10.1029/2010GL046402, http://doi.wiley.com/10.1029/2010GL046402, 2011.

Langford, A. O. and Reid, S. J.: Dissipation and mixing of a small-scale stratospheric intrusion in the upper troposphere, Journal of Geophysical Research Atmospheres, 103, 31 265–31 276, https://doi.org/10.1029/98JD02596, 1998.

Meinshausen, M., Smith, S. J., Calvin, K., Daniel, J. S., Kainuma, M. L. T., Lamarque, J.-F., Matsumoto, K., Montzka, S. A., Raper, S. C. B., Riahi, K., Thomson, A., Velders, G. J. M., and van Vuuren, D. P.: The RCP greenhouse gas concentrations and their extensions from 1765 to 2300, Climatic Change, 109, 213–241, https://doi.org/10.1007/s10584-011-0156-z, http://link.springer.com/10.1007/s10584-011-0156-z, 2011.

Meul, S., Langematz, U., Kröger, P., Oberländer-Hayn, S., and Jöckel, P.: Future changes in the stratosphere-to-troposphere ozone mass flux and the contribution from climate change and ozone recovery, Atmospheric Chemistry and Physics, 18, 7721–7738, https://doi.org/10.5194/acp-18-7721-2018, 2018.

Morgenstern, O., Hegglin, M. I., Rozanov, E., O'Connor, F. M., Abraham, N. L., Akiyoshi, H., Archibald, A. T., Bekki, S., Butchart, N., Chipperfield, M. P., Deushi, M., Dhomse, S. S., Garcia, R. R., Hardiman, S. C., Horowitz, L. W., Jöckel, P., Josse, B., Kinnison, D., Lin, M., Mancini, E., Manyin, M. E., Marchand, M., Marécal, V., Michou, M., Oman, L. D., Pitari, G., Plummer, D. A., Revell, L. E., Saint-Martin, D., Schofield, R., Stenke, A., Stone, K., Sudo, K., Tanaka, T. Y., Tilmes, S., Yamashita, Y., Yoshida, K., and Zeng, G.: Review of the global models used within phase 1 of the Chemistry–Climate Model Initiative (CCMI), Geoscientific Model Development, 10, 639–671, https://doi.org/10.5194/gmd-10-639-2017, https://www.geosci-model-dev.net/10/639/2017/, 2017.

Morgenstern, O., Stone, K. A., Schofield, R., Akiyoshi, H., Yamashita, Y., Kinnison, D. E., Garcia, R. R., Sudo, K., Plummer, D. A., Scinocca, J., Oman, L. D., Manyin, M. E., Zeng, G., Rozanov, E., Stenke, A., Revell, L. E., Pitari, G., Mancini, E., DI Genova, G., Visioni, D., Dhomse, S. S., and Chipperfield, M. P.: Ozone sensitivity to varying greenhouse gases and ozone-depleting substances in CCMI-1 simulations, Atmospheric Chemistry and Physics, 18, 1091–1114, https://doi.org/10.5194/acp-18-1091-2018, 2018.

Nakicenovic, N., Alcamo, J., Grubler, A., Riahi, K., Roehrl, R., Rogner, H.-H., and Victor, N.: IPCC Special Report on Emissions Scenarios: A special report of Working Group III of the Intergovernmental Panel on Climate Change, Cambridge University Press, https://doi.org/92-9169-113-5, http://pure.iiasa.ac.at/id/eprint/6101/, 2000.

Neu, J. L., Flury, T., Manney, G. L., Santee, M. L., Livesey, N. J., and Worden, J.: Tropospheric ozone variations governed by changes in stratospheric circulation, Nature Geoscience, 7, 340–344, https://doi.org/10.1038/ngeo2138, http://www.nature.com/ngeo/journal/v7/n5/full/ngeo2138.html{%}5Cnhttp://www.nature.com/ngeo/journal/v7/n5/pdf/ngeo2138.pdf, 2014.

Oberländer-Hayn, S., Gerber, E. P., Abalichin, J., Akiyoshi, H., Kerschbaumer, A., Kubin, A., Kunze, M., Langematz, U., Meul, S., Michou, M., Morgenstern, O., and Oman, L. D.: Is the Brewer-Dobson circulation increasing or moving upward?, Geophysical Research Letters, 43, 1772–1779, https://doi.org/10.1002/2015GL067545, 2016.

Orbe, C., Yang, H., Waugh, D. W., Zeng, G., Morgenstern, O., Kinnison, D. E., Lamarque, J. F., Tilmes, S., Plummer, D. A., Scinocca, J. F., Josse, B., Marecal, V., Jöckel, P., Oman, L. D., Strahan, S. E., Deushi, M., Tanaka, T. Y., Yoshida, K., Akiyoshi, H., Yamashita,

Y., Stenke, A., Revell, L., Sukhodolov, T., Rozanov, E., Pitari, G., Visioni, D., Stone, K. A., Schofield, R., and Banerjee, A.: Large-scale tropospheric transport in the Chemistry-Climate Model Initiative (CCMI) simulations, Atmospheric Chemistry and Physics, 18, 7217–7235, https://doi.org/10.5194/acp-18-7217-2018, 2018.

Polvani, L. M., Abalos, M., Garcia, R., Kinnison, D., and Randel, W. J.: Significant Weakening of Brewer-Dobson Circulation Trends Over the 21st Century as a Consequence of the Montreal Protocol, Geophysical Research Letters, 45, 401–409, https://doi.org/10.1002/2017GL075345, http://doi.wiley.com/10.1002/2017GL075345, 2018.

Polvani, L. M., Wang, L., Abalos, M., Butchart, N., Chipperfield, M. P., Dameris, M., Deushi, M., Dhomse, S. S., Jöckel, P., Kinnison, D., Michou, M., Morgenstern, O., Oman, L. D., Plummer, D. A., and Stone, K. A.: Large Impacts, Past and Future, of Ozone-Depleting Substances on Brewer-Dobson Circulation Trends: A Multimodel Assessment, Journal of Geophysical Research: Atmospheres, 124, 6669–6680, https://doi.org/10.1029/2018JD029516, 2019.

Ramaswamy, V., Chanin, M. L., Angell, J., Barnett, J., Gaffen, D., Gelman, M., Keckhut, P., Koshelkov, Y., Labitzke, K., Lin, O'Neill, a., Nash, J., Randel, W., Rood, R., Shine, K., Shiotani, M., and Swinbank, R.: Stratospheric temperature trends: Observations and model simulations, Rev. Geophys., 39, 71–122, https://doi.org/10.1029/1999rg000065, http://dx.doi.org/10.1029/1999rg000065{%}5Cnpapers2://publication/doi/10.1029/1999rg000065, 2001.

Revell, L. E., Tummon, F., Stenke, A., Sukhodolov, T., Coulon, A., Rozanov, E., Garny, H., Grewe, V., and Peter, T.: Drivers of the tropospheric ozone budget throughout the 21st century under the medium-high climate scenario RCP 6.0, Atmospheric Chemistry and Physics, 15, 5887–5902, https://doi.org/10.5194/acp-15-5887-2015, 2015.

Rind, D., Lerner, J., and McLinden, C.: Changes of tracer distributions in the doubled CO2 climate, Journal of Geophysical Research-Atmospheres, 106, 28 061–28 079, https://doi.org/10.1029/2001JD000439, 2001.

Sekiya, T. and Sudo, K.: Roles of transport and chemistry processes in global ozone change on interannual and multidecadal time scales, Journal of Geophysical Research, 119, 4903–4921, https://doi.org/10.1002/2013JD020838, 2014.

Shapiro, M. A.: Turbulent Mixing within Tropopause Folds as a Mechanism for the Exchange of Chemical Constituents between the Stratosphere and Troposphere, https://doi.org/10.1175/1520-0469(1980)037<0994:TMWTFA>2.0.CO;2, http://journals.ametsoc.org/doi/abs/10.1175/1520-0469{%}281980{%}2937{%}3C0994{%}3ATMWTFA{%}3E2.0.CO{%}3B2, 1980.

Škerlak, B., Sprenger, M., and Wernli, H.: A global climatology of stratosphere-troposphere exchange using the ERA-Interim data set from 1979 to 2011, Atmospheric Chemistry and Physics, 14, 913–937, https://doi.org/10.5194/acp-14-913-2014, 2014.

Sprenger, M., Maspoli, M. C., and Wernli, H.: Tropopause folds and cross-tropopause exchange: A global investigation based upon ECMWF analyses for the time period March 2000 to February 2001, Journal of Geophysical Research Atmospheres, 108, 1–11, https://doi.org/10.1029/2002jd002587, 2003.

Stevenson, D. S., Young, P. J., Naik, V., Lamarque, J. F., Shindell, D. T., Voulgarakis, A., Skeie, R. B., Dalsoren, S. B., Myhre, G., Berntsen, T. K., Folberth, G. A., Rumbold, S. T., Collins, W. J., MacKenzie, I. A., Doherty, R. M., Zeng, G., Van Noije, T. P., Strunk, A., Bergmann, D., Cameron-Smith, P., Plummer, D. A., Strode, S. A., Horowitz, L., Lee, Y. H., Szopa, S., Sudo, K., Nagashima, T., Josse, B., Cionni, I., Righi, M., Eyring, V., Conley, A., Bowman, K. W., Wild, O., and Archibald, A.: Tropospheric ozone changes, radiative forcing and attribution to emissions in the Atmospheric Chemistry and Climate Model Intercomparison Project (ACCMIP), Atmospheric Chemistry and Physics, 13, 3063–3085, https://doi.org/10.5194/acp-13-3063-2013, 2013.

Stohl, A., Bonasoni, P., Cristofanelli, P., Collins, W., Feichter, J., Frank, A., Forster, C., Gerasopoulos, E., Gäggeler, H., James, P., Kentarchos, T., Kreipl, S., Kromp-Kolb, H., Krüger, B., Land, C., Meloen, J., Papayannis, A., Priller, A., Seibert, P., Sprenger, M., Roelofs,

G. J., Scheel, E., Schnabel, C., Siegmund, P., Tobler, L., Trickl, T., Wernli, H., Wirth, V., Zanis, P., and Zerefos, C.: Stratosphere-troposphere exchange - a review, and what we have learned from STACCATO, Journal of Geophysical Research: Atmospheres, 108, 8516, https://doi.org/10.1029/2002JD002490, http://dx.doi.org/10.1029/2002JD002490, 2003.

Storch, H. V. and Zwiers, F. W.: Statistical Analysis in Climate Research, Journal of the American Statistical Association, 95, 1375, https://doi.org/10.1017/CBO9780511612336, http://ebooks.cambridge.org/ref/id/CBO9780511612336, 1999.

Sudo, K., Takahashi, M., and Akimoto, H.: Future changes in stratosphere-troposphere exchange and their impacts on future tropospheric ozone simulations, Geophysical Research Letters, 30, 2256, https://doi.org/10.1029/2003GL018526, 2003.

Vallis, G. K., Zurita-Gotor, P., Cairns, C., and Kidston, J.: Response of the large-scale structure of the atmosphere to global warming, Quarterly Journal of the Royal Meteorological Society, 141, 1479–1501, https://doi.org/10.1002/qj.2456, 2015.

Waugh, D. W. and Polvani, L. M.: Climatology of intrusions into the tropical upper troposphere, Geophysical Research Letters, 27, 3857–3860, https://doi.org/10.1029/2000GL012250, 2000.

Waugh, D. W., Grise, K. M., Seviour, W. J. M., Davis, S. M., Davis, N., Adam, O., Son, S.-W., Simpson, I. R., Staten, P. W., Maycock, A. C., Ummenhofer, C. C., Birner, T., Ming, A., Waugh, D. W., Grise, K. M., Seviour, W. J. M., Davis, S. M., Davis, N., Adam, O., Son, S.-W., Simpson, I. R., Staten, P. W., Maycock, A. C., Ummenhofer, C. C., Birner, T., and Ming, A.: Revisiting the Relationship among Metrics of Tropical Expansion, Journal of Climate, 31, 7565–7581, https://doi.org/10.1175/JCLI-D-18-0108.1, http://journals.ametsoc.org/doi/10.1175/JCLI-D-18-0108.1, 2018.

Wernli, H. and Sprenger, M.: Identification and ERA-15 Climatology of Potential Vorticity Streamers and Cutoffs near the Extratropical Tropopause, Journal of the Atmospheric Sciences, 64, 1569–1586, https://doi.org/10.1175/JAS3912.1, http://journals.ametsoc.org/doi/abs/10.1175/JAS3912.1, 2007.

WHO: Health Aspects of Air Pollution with Particulate Matter, Ozone and Nitrogen Dioxide Report on a WHO Working Group OZONE-adverse effects NITROGEN DIOXIDE-adverse effects AIR POLLUTANTS, ENVIRONMENTAL-adverse effects META-ANALYSIS AIR-standards GUIDELINES, p. 30, http://www.euro.who.int/{_}{_}data/assets/pdf{_}file/0005/112199/E79097.pdf, 2003.

WMO: Scientific Assessment of Ozone Depletion: 2018, Global Ozone Research and Monitoring Project–Report, 58, Geneva, Switzerland, 2018.

Yang, H., Chen, G., Tang, Q., and Hess, P.: Quantifying isentropic stratosphere-troposphere exchange of ozone, Journal of Geophysical Research: Atmospheres, 121, 3372–3387, https://doi.org/10.1002/2015JD024180, 2016.

Zeng, G. and Pyle, J. A.: Changes in tropospheric ozone between 2000 and 2100 modeled in a chemistry-climate model, Geophysical Research Letters, 30, https://doi.org/10.1029/2002GL016708, http://doi.wiley.com/10.1029/2002GL016708, 2003.

Zeng, G., Morgenstern, O., Braesicke, P., and Pyle, J. A.: Impact of stratospheric ozone recovery on tropospheric ozone and its budget, Geophysical Research Letters, 37, n/a–n/a, https://doi.org/10.1029/2010GL042812, http://doi.wiley.com/10.1029/2010GL042812, 2010.

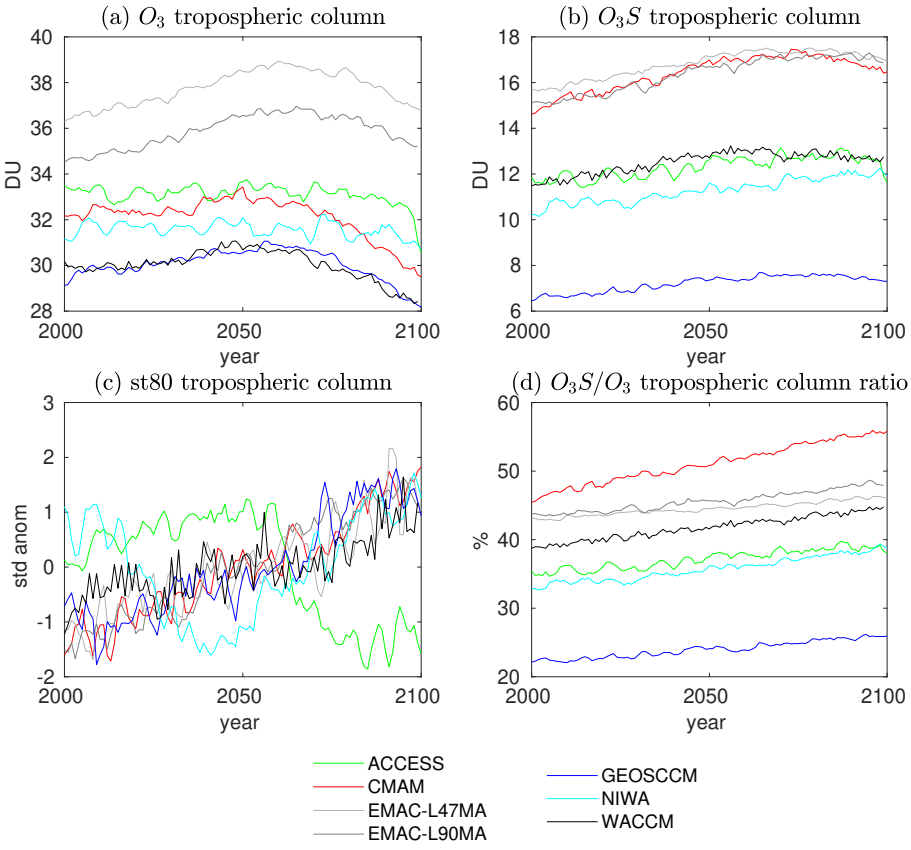

Figure 1. Time series of tropospheric columns of ozone (a), stratospheric ozone (b), st80 (c) and the ratio between O_3 and O_3S (d). Ozone and stratospheric ozone are plotted in Dobson units, while st80 is shown as standardized anomalies (removing the mean and dividing by the standard deviation).

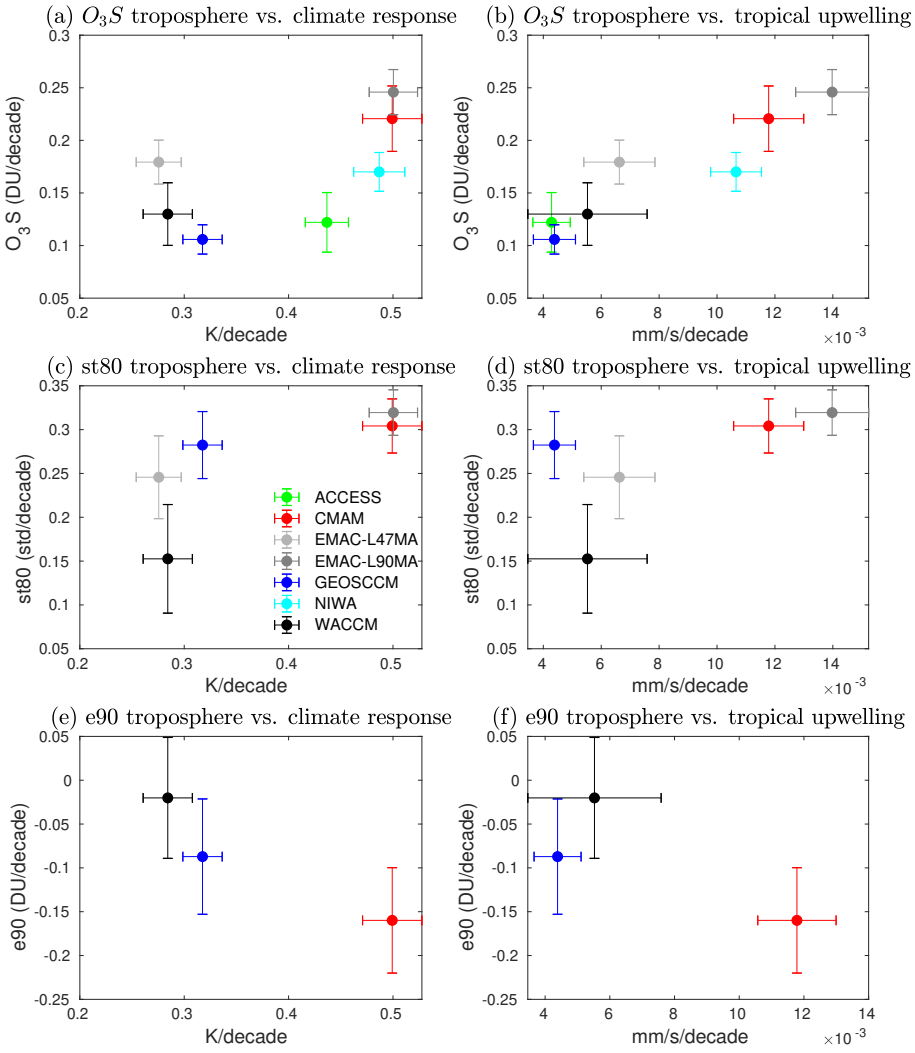

Figure 2. Trends over the 21st century in globally integrated tropospheric columns of idealized tracers ~~versus~~ (a and b: O_3, c and d: st80, e and f: e90) plotted against model climate response (a, ~~b~~c and e) and against tropical upwelling (b, d and f). Climate response is evaluated as the tropical upper tropospheric temperature trends (30S-30N and 400-150 hPa)~~.~~, tropical upwelling is averaged over 100-70 hPa and ~~versus globally integrated tropopause rise (c, d). Panel (c) shows tropopause rise as a function of climate response~~ 20S-20N. The error bars represent the trend uncertainty calculated with a Student t test with a 95% confidence level.

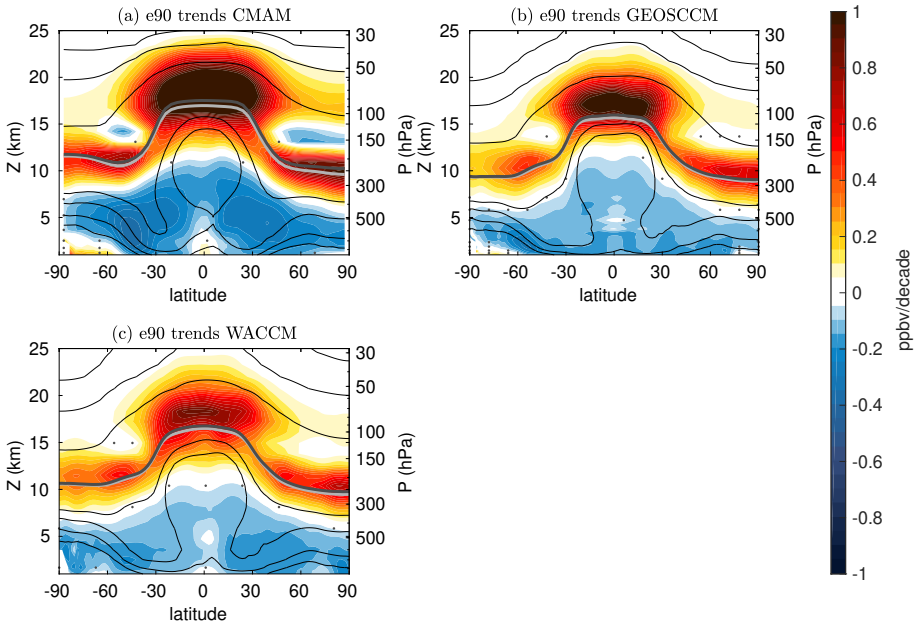

Figure 3. Trends over the 21st century in e90 (ppbv/decade). The dotted regions indicate where the trends are not statistically significant for a 95% confidence level. The light and dark gray lines indicate the location of the tropopause in the first and last 10 years of the 21st century, respectively. Thin black contours show the climatological concentrations of e90 (contour levels [0.1 1 10 100 110 120 130] ppbv). Note that Z is the log-pressure altitude $Z = Hln(p_0/p)$, with H=7 km and p_0=1000 hPa in this figure and in all other cross-sections.

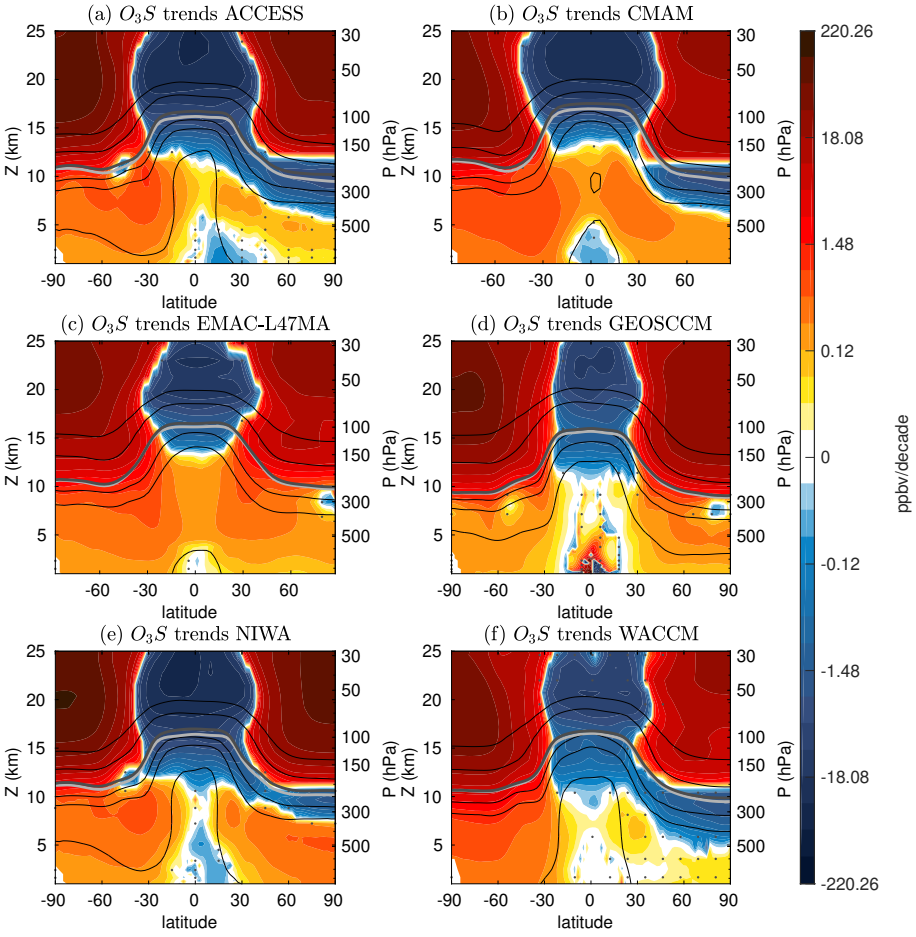

Figure 4. Trends over the 21st century in stratospheric ozone (ppmv/decade, in logarithmic scale). The dotted regions indicate where the trends are not statistically significant for a 95% confidence level. The light and dark gray lines indicate the location of the tropopause in the first and last 10 years of the 21st century, respectively. Thin black contours show the climatological concentrations of O_3S (contour levels [10 50 100 500 1000] ppbv).

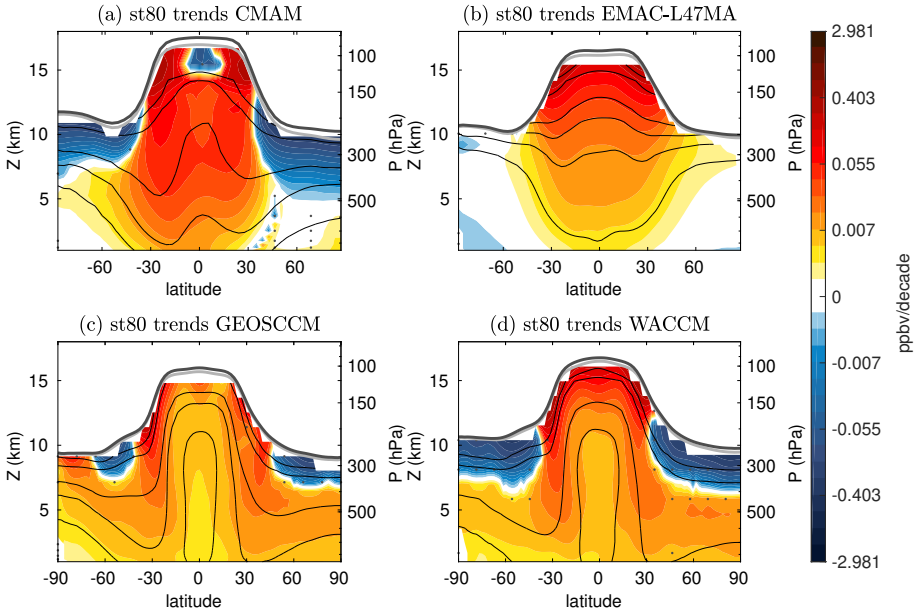

Figure 5. Trends over the 21st century in stratospheric tracer st80 (ppbv/day, in logarithmic scale). The dotted regions indicate where the trends are not statistically significant for a 95% confidence level. The light and dark gray lines indicate the location of the tropopause in the first and last 10 years of the 21st century, respectively. Thin black contours show the climatological concentrations of st80 (contour levels [0.1 0.25 0.5 1 5 10] ppbv.

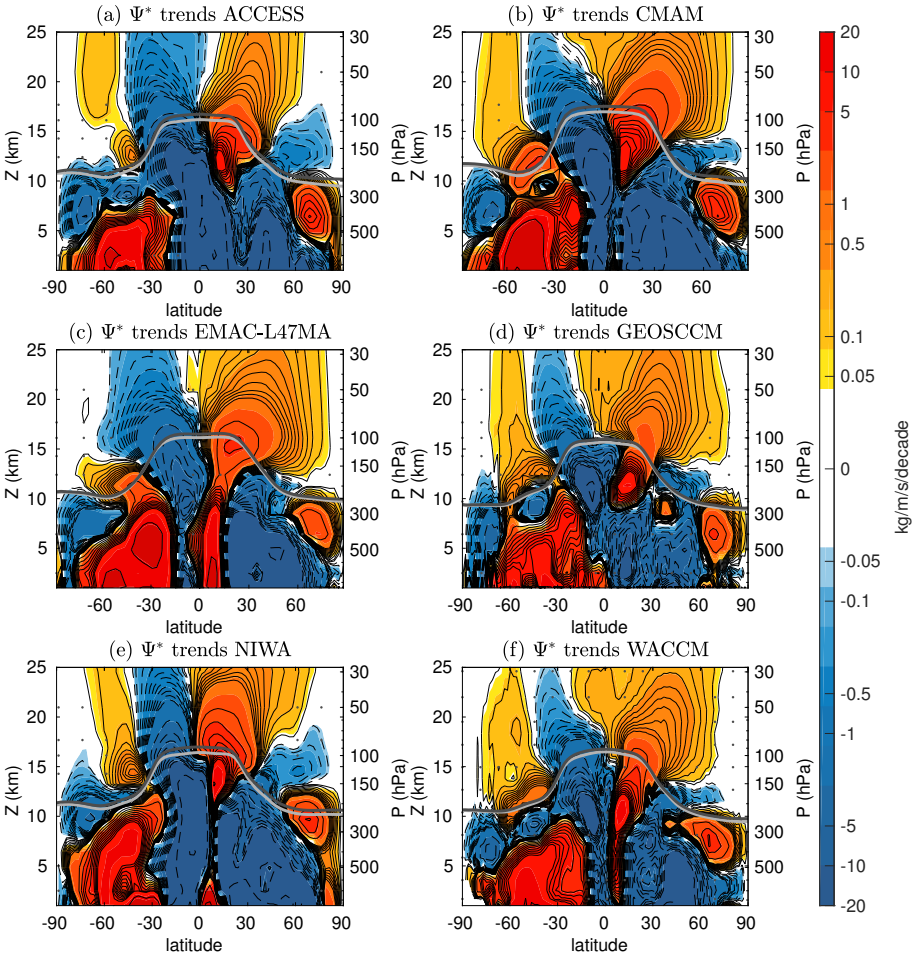

Figure 6. Trends over the 21st century in residual circulation streamfunction. The dotted regions indicate where the trends are not statistically significant for a 95% confidence level. The light and dark gray lines indicate the location of the tropopause in the first and last 10 years of the 21st century, respectively.

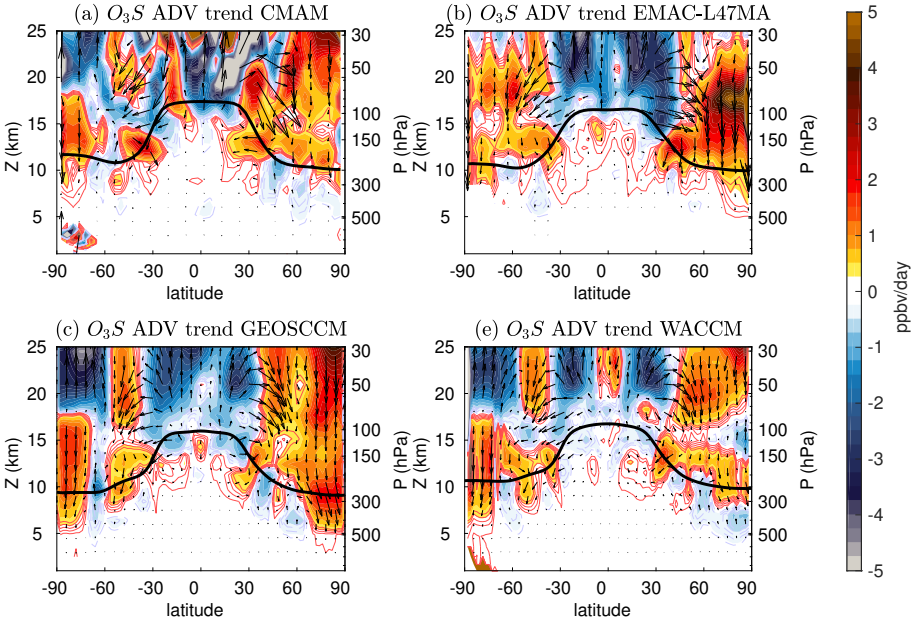

Figure 7. Change over the 21st century in the O_3S TEM advective transport term (shading, ppbv/day) in CMAM (a), EMAC-L47MA (b), GEOSCCM (c) and WACCM (d). The arrows show the residual circulation components multiplied by the absolute value of the corresponding tracer gradient.

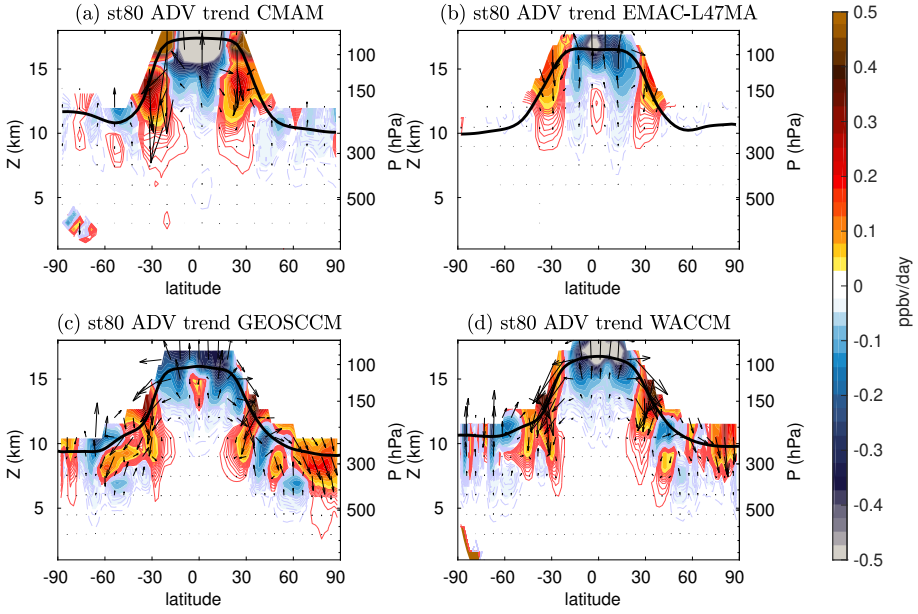

Figure 8. Change over the 21st century in the st80 TEM advective transport term (shading, ppbv/day) in CMAM (a), EMAC-L47MA (b), GEOSCCM (c) and WACCM (d). The arrows show the residual circulation components multiplied by the absolute value of the corresponding tracer gradient.

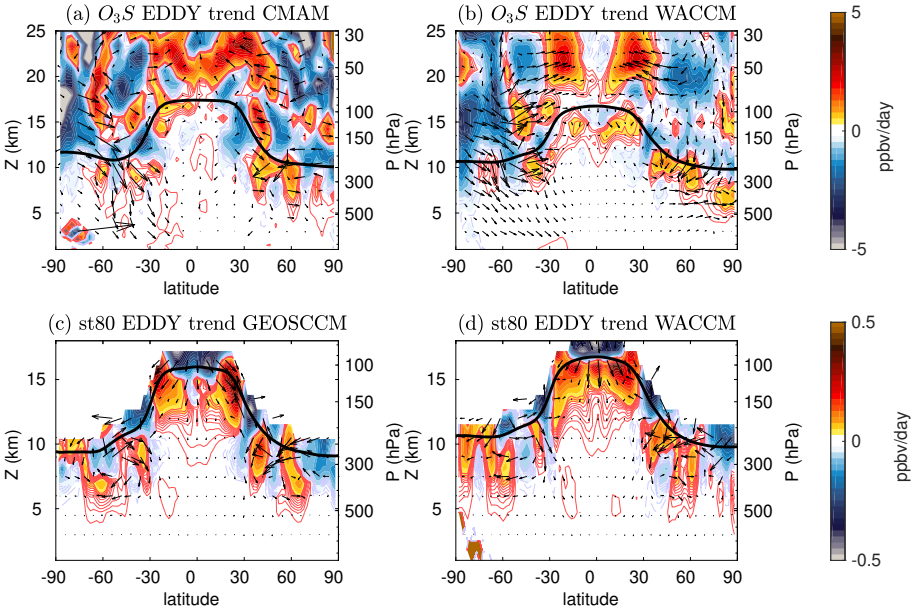

Figure 9. Change over the 21st century in the st80 TEM eddy transport term (shading, ppbv/day) in CMAM (a), EMAC-L47MA (b), GEOSCCM (c) and WACCM (d). Arrows denote the direction of the eddy tracer flux.

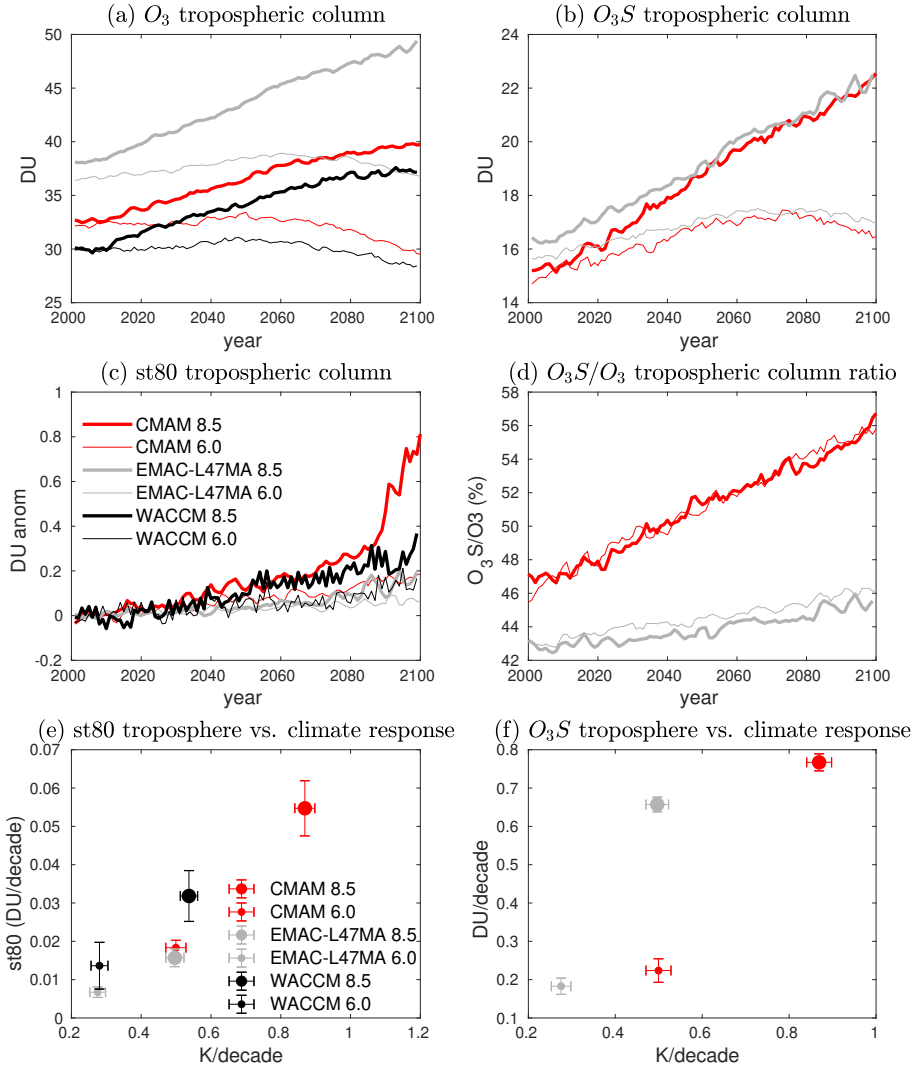

Figure 10. Panels a-d: Timeseries in tropospheric column tracers for the RCP8.5 ~~scenario~~(thick lines) and RCP 6.0 (thin lines) scenarios. The st80 concentrations are expressed as anomalies with respect to the average of the first ten years, and the values for EMAC-L47MA are multiplied by an arbitrary factor of 50 (see text for details). Panels e and f: Trends in tropospheric column tracers versus model climate response for the RCP8.5 (large circles) and the RCP6.0 (~~stars~~small circles) ~~emission~~ scenarios. The error bars represent the trend uncertainty with a 95% confidence level. Note that the O_3S tracer is not available in the RCP8.5 WACCM simulation.

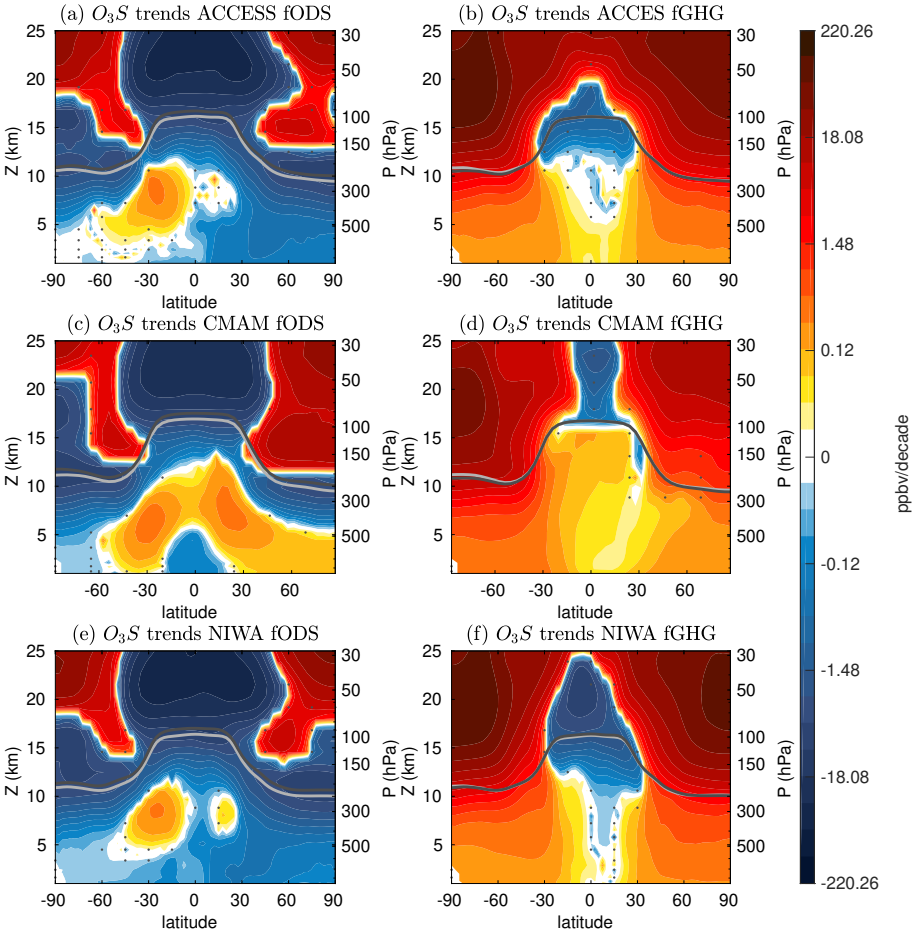

Figure 11. Trends over the 21st century in O_3S (ppbv/decade) for the simulations with ODS (a, b) or GHG (c, d) concentrations fixed to 1960 levels in ACCESS (a, c) and CMAM (b, d). The dotted regions indicate where the trends are not statistically significant for a 95% confidence level. The light and dark gray lines indicate the location of the tropopause in the first and last 10 years of the 21st century, respectively.

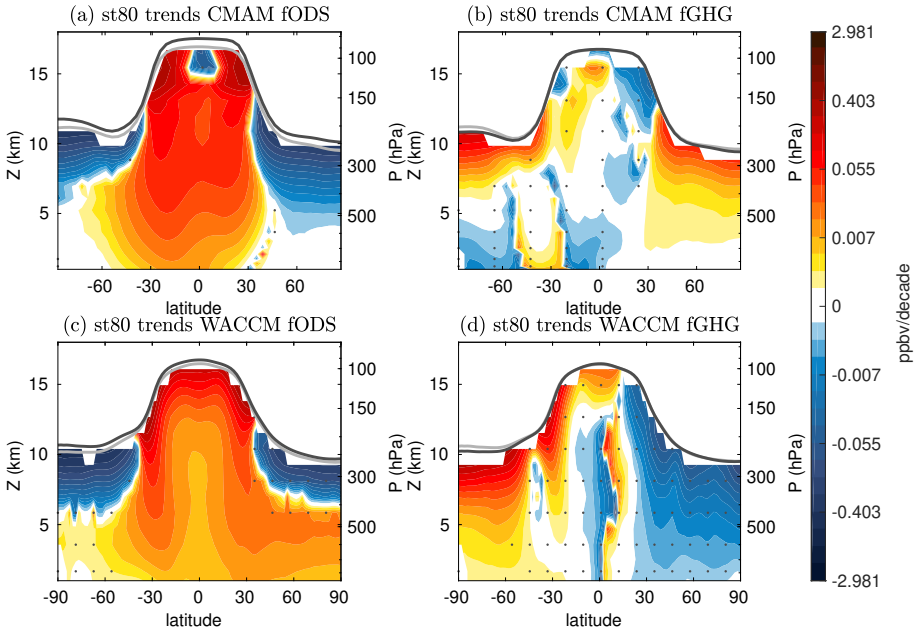

Figure 12. Trends over the 21st century in st80 for the simulations with ODS (a, b) or GHG (c, d) concentrations fixed to 1960 levels in CMAM (a, c) and WACCM (b, d). The dotted regions indicate where the trends are not statistically significant for a 95% confidence level. The light and dark gray lines indicate the location of the tropopause in the first and last 10 years of the 21st century, respectively.